Genomic characterisation of brain malignancies through liquid biopsies: The cerebrospinal fluid-derived circulating tumour DNA better represents the genomic alterations of brain tumours than plasma

Leticia De Mattos Arruda

Genomic characterisation of brain malignancies through liquid biopsies:

The cerebrospinal fluid-derived circulating tumour DNA better represents the genomic alterations of brain tumours than plasma

Doctoral thesis at the Universitat Autònoma de Barcelona (UAB), Doctoral Program in Medicine, Department of Medicine of UAB
for obtaining the academic degree of **Doctor of Philosophy**

Leticia De Mattos Arruda, MD, Master UAB 2012-2013

Directors:
Joan Seoane, PhD
Javier Cortes, MD, PhD

Tutor:
Josep Angel Bosch Gil, MD, PhD

Vall d'Hebron Institute of Oncology / Vall d'Hebron University Hospital
Barcelona, Spain

Barcelona, March 2016

Acknowledgements

I would like to express my special appreciation and thanks to my thesis directors Professor Joan Seoane and Dr Javier Cortes. I would like to thank them for encouraging my research and for allowing me to grow as a clinician scientist. Their advice on both research as well as on my career have been inestimable.

I would also like to thank my tutor, Dr. Josep Angel Bosch Gil, for making the interaction with the university possible; and Dr. Josep Tabernero, for unrestrictive support during this journey.

I wish to express my warmest gratitude to all those colleagues and advisors whose comments, criticisms, support and encouragement, personal and academic, have left a mark on this work. I also wish to thank those institutions – Memorial Sloan Kettering Cancer Center and Cancer Research UK Cambridge Institute that have supported me during the work on this thesis.

I would especially like to thank physicians, scientists, post-docs, technicians, nurses, study coordinators, and assistants at the Vall d'Hebron Institute of Oncology / Vall d'Hebron University Hospital and specially the departments of Medical Oncology/ Breast Cancer Unit/ Phase I Unit, Neurosurgery, Pathology and Prof Seoane's laboratory staff for the remarkable support when we designed of the project, recruited patients, collected data, performed the experiments and interpreted the data.

There aren't enough words to express how grateful I am to my mother, father, brother and sister and grandmothers. I would also like to thank all of my friends who supported me, and encouraged me to strive towards my goals.

Table of contents

Chapter 1: Introduction

Cell-free tumour DNA

In medical oncology, the next generation or massively parallel sequencing of tumour tissue biopsies in search of actionable somatic genomic alterations has become routine practice. Although the information derived from tumour tissue biopsies can be informative, the procurement of tumour tissue specimens poses challenges for the development of biomarkers. Tumour biopsies are single portraits of the tumour in time, can be difficult to obtain, can be costly and time consuming, and subject to selection bias resulting from tumour heterogeneity (1, 2).

Blood-based circulating biomarkers, including circulating tumour cells (CTCs), cell-free nucleic acids and exosomes, have been studied as 'liquid biopsies', that is, surrogates or complementary biomarkers to overcome the drawbacks of invasive tissue biopsies (3). Recent developments in massively parallel sequencing and digital genomic techniques have allowed for interrogation of tumour-specific molecular alterations in the circulation and support the clinical validity of cell-free circulating tumour DNA (ctDNA) as a liquid biopsy in human cancer (4-17).

Plasma is known to carry small amounts of fragmented cell-free DNA of 160 to 180 base pairs, which is likely to be originated from cancer cells through the process of necrosis and apoptosis (18-20). Tumour-derived DNA is defined by the presence of genomic alterations, and can be discerned from normal DNA, reassuring the specificity of these liquid biopsies as biomarkers in cancer (20). CtDNA in plasma constitutes a non-invasive source of material that may allow the identification of the genomic make-up of tumours and provides a new means for studying cancer patients in terms of monitoring tumour burden, assessing the mechanisms of therapeutic response and resistance, detecting minimal residual disease, and understanding unresolved biologic puzzles presented by tumour heterogeneity and clonal evolution (4-17).

We have reported a proof-of-principle study in the field of liquid biopsies, which is going to be an ancillary article analysed in this thesis entitled: "***Capturing intra-tumour genetic heterogeneity by de novo mutation profiling of circulating cell-free tumour DNA: a proof-of-principle*" (10)** published in *Annals of Oncology* in July 2014. This article is one of the first to demonstrate that high-depth targeted massively parallel sequencing of plasma-derived ctDNA constitutes a potential tool for *de novo* mutation identification and monitoring of somatic genomic alterations during the course of targeted therapy, and this non-invasive tool may be employed to overcome the challenges posed by tumour heterogeneity.

The need of liquid biopsies in brain malignancies

Brain malignancies are associated with dismal outcomes with few therapeutic options available. Glioblastomas (GBMs) are highly malignant, usually recalcitrant to radiotherapy and chemotherapy and exhibit a dismal prognosis (21). GBMs are characterised by an extremely invasive nature resulting in the inability of surgery to completely eradicate tumours.

Likewise, secondary brain malignancies (i.e., brain metastasis from solid cancers) are a devastating complication of cancer with also unmet therapeutic needs. The development of brain metastasis is an important clinical challenge associated with poor prognosis, neurological deterioration, and reduced quality of life (22). Despite the recent success of some therapies in the treatment of extracranial diseases, the outcome of patients developing brain metastasis has not been improved (23).

In brain malignancies, the development of non-invasive methods to analyse the characteristics of tumours is paramount. The restricted and invasive accesses for sampling brain tumour material and the difficulties to capture the heterogeneous and evolving nature of this type of tumours through the analysis of small fragments of tumour represent main obstacles for their genomic characterisation (21, 24, 25).

In patients with primary and secondary brain malignancies, the repeated tumour sampling and limited abundance of brain tumour-derived ctDNA in the plasma makes the use of liquid biopsy challenging yet. In patients with primary brain tumours, the presence of ctDNA derived from plasma is minimal probably as a result of the blood-brain barrier (12, 26, 27), although proof-of-principle studies have suggested the release of CTCs into the circulation of GBM patients (28-30).

The cerebrospinal fluid (CSF) is a liquid that bathes the central nervous system (CNS) and is in intimate contact with tumour and normal cells in CNS malignancies (31, 32). Recently, there has been preliminary evidence that tumour-derived DNA is present in the CSF of patients with brain malignancies (31-35).

However, the extension to how brain tumour-derived ctDNA represents the tumour clonal diversity as compared with plasma ctDNA from the same patients with primary and secondary brain malignancies, and how ctDNA from CSF or plasma recapitulates multiregional SNC and extra-cranial tumour samples has not been explored.

We have reported a proof-of-principle in the field of CNS liquid biopsies, which is going to be the fundamental article analysed for this thesis entitled: **“Cerebrospinal fluid-derived circulating tumour DNA better represents the genomic alterations of brain tumours than plasma” (14)** published in *Nature Communications* in November 2015**.**

Chapter 2: Capturing intra-tumour genetic heterogeneity by *de novo* mutation profiling of circulating cell-free tumour DNA: a proof-of-principle

Introduction

Breast cancers are genomically heterogeneous. In breast, akin to other solid tumours, the collection of genomic alterations found within a given tumour may differ according to the region sampled, between primary tumour and metastatic deposits, and even between distinct metastatic deposits (10, 36-38). The genomic analyses of breast cancers have provided direct evidence of spatial and temporal intra-tumour heterogeneity (39-41) and have shown that the range of subclonal heterogeneity is variable among breast cancers (38).

Currently, clinical and therapeutic decisions are usually based on individual biopsies that may not be representative of the entire tumour burden or not real-time assessments of the tumour tissue (2). The clinic goals for understanding tumour heterogeneity consist on i) characterising the cancers of patients and guiding their treatment, and ii) monitoring the emergence of drug resistance and selecting tailored therapies. However, these goals cannot be accomplished with the current mode of analyses of tumour tissue biopsies.

Liquid biopsies, particularly plasma ctDNA, may help to overcome the challenges of tumour heterogeneity and sampling bias derived from the analysis of single biopsies. In addition, they may be suitable for revealing actionable genomic alterations and informing the decision-making processes in the clinic.

In this work (10), we hypothesised that massively parallel sequencing analysis of plasma-derived ctDNA of breast cancer patient would constitute a means to identify the repertoire of genomic alterations between primary tumour and metastasis and also to monitor the presence of potentially actionable driver somatic genomic alterations during the course of targeted therapy **(Figure 2.1)**.

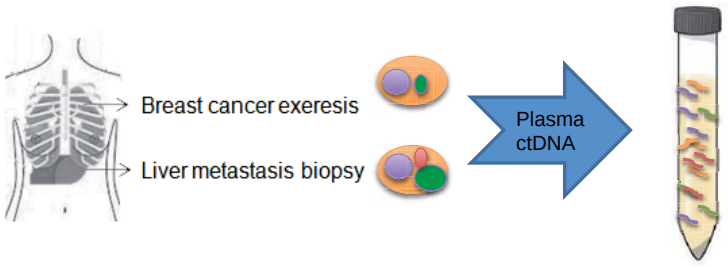

Figure 2.1. Schematics for the role of plasma-derived ctDNA capturing mutations for both primary tumour and metastasis.

Objectives

- Assess whether plasma-derived ctDNA could be a potential surrogate for tumour DNA obtained from tissue biopsies.
- Assess whether the analysis of plasma-derived ctDNA could be useful to monitor actionable driver somatic genomic alterations during the course of targeted therapy.

Results

A 66-year-old patient presented with synchronous oestrogen receptor (ER)-positive/ HER2-negative, highly proliferative, grade 2, mixed invasive ductal-lobular carcinoma with bone and liver metastases at diagnosis **(Appendices Figure A1)**. Following three lines of chemotherapy (i.e. paclitaxel-, anthracycline- and capecitabine-based therapies and disease progression, the patient underwent a molecular pre-screening program **(Figure 2.2)**. The analysis of archival primary breast tumour material by Sequenom MassARRAY® revealed the presence of an *AKT1* E17K mutation. Based on these results, the patient was enrolled in the phase I study PAM4743g (Clinicaltrials.gov, NCT01090960) and treated with Ipatasertib (GDC-0068), a highly selective, orally available pan-AKT inhibitor as the fourth line of therapy. Multiple plasma samples were collected during the fourth line of treatment with an AKT inhibitor.

DNA extracted from archival tumour material and plasma, and from peripheral blood leukocytes was subjected to targeted massively parallel sequencing at the Integrated Genomics Operation (iGO), Memorial Sloan Kettering Cancer Center (MSKCC) using the Integrated Mutation Profiling of Actionable Cancer Targets (IMPACT) platform (42), comprising 300 cancer genes known to harbour actionable mutations **(Appendices Supplementary Data 1)**.

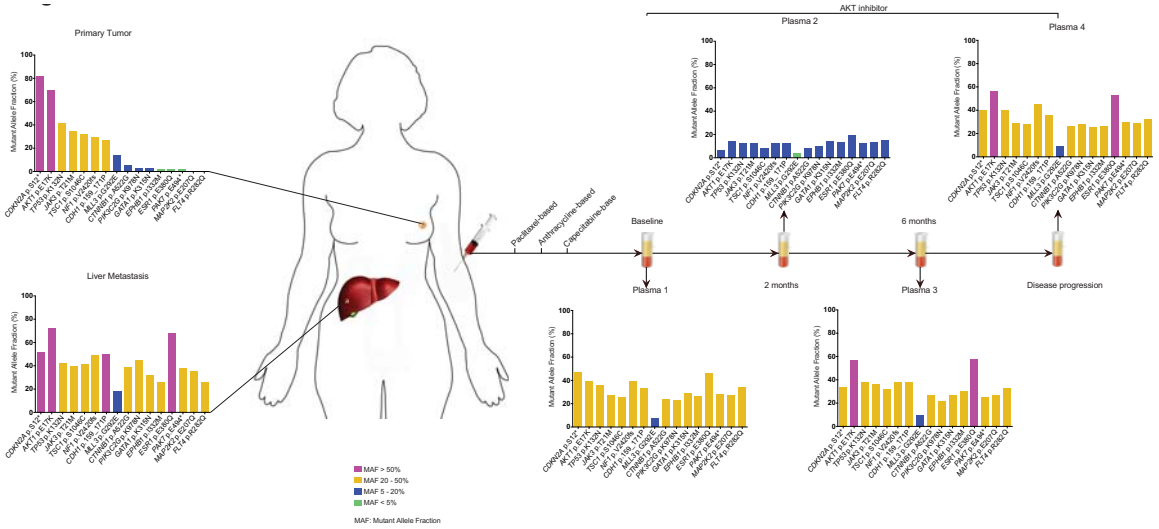

Figure 2.2. Patient disease presentation, treatment timeline and mutant alleles in the primary breast tumour, liver metastasis and plasma-derived DNA. Biopsies of the primary breast cancer and its synchronous liver metastasis were obtained before initiation of therapy. Following three lines of chemotherapy, the patient was treated with the AKT inhibitor Ipatasertib, and multiple plasma samples were obtained during the course of treatment. DNA samples extracted from the primary tumour, metastasis and plasma samples were subjected to targeted high-depth massively parallel sequencing.

Average read depths of 287x were obtained from the archival primary tumour, 139x from the liver metastasis and between 200x and 900x from the ctDNA samples. Sixteen somatic non-synonymous mutations were detected in the liver metastasis, of which 9 (*CDKN2A*, *AKT1*, *TP53*, *JAK3*, *TSC1*, *NF1*, *CDH1*, *MML3* and *CTNNB1*) were also detected in >5% of the alleles found in the primary tumour sample.

Not all mutations identified in the liver metastasis were reliably identified in the primary tumour (e.g. *FLT4, MAP2K2*) at the sequencing depth obtained. Analysis of plasma ctDNA, nevertheless, captured all mutations present in the primary breast tumour and/ or synchronous liver metastasis **(Figure 2.2, Figure 2.3 and Table 2.1)**.

Gene	Mutation (amino acid)	Primary tumor (287x) MAFs (reads)	Liver metastasis (139x) MAFs (reads)	Plasma 1 (692x) MAFs (reads)	Plasma 2 (728x) MAFs (reads)	Plasma 3 (209x) MAFs (reads)	Plasma 4 (918x) MAFs (reads)
CDKN2A	p.S12*	82% (23/28)	52% (11/21)	47% (42/89)	6% (7/117)	34% (14/41)	40% (55/137)
AKT1	p.E17K	70% (83/118)	72% (79/110)	39% (204/521)	14% (83/593)	57% (100/174)	56% (373/663)
TP53	p.K132N	42% (101/241)	42% (48/113)	36% (228/625)	12% (92/753)	38% (78/204)	40% (339/841)
JAK3	p.T21M	35% (60/172)	40% (56/141)	27% (253/939)	12% (100/834)	36% (122/340)	29% (343/1181)
TSC1	p.S1046C	32% (31/98)	41% (55/134)	25% (132/521)	8% (43/518)	32% (59/182)	28% (179/636)
NF1	p.V2420fs	30% (153/511)	49% (61/124)	39% (186/483)	12% (92/761)	38% (49/159)	45% (328/726)
CDH1	p.159_171 PPISCPENEKGPF>L	27% (56/210)	50% (46/92)	33% (197/605)	12% (93/758)	38% (52/138)	36% (265/731)
MLL3	p.G292E	14% (64/446)	18% (30/168)	7% (67/1002)	4% (48/1183)	9% (31/352)	9% (73/831)
CTNNB1	p.A522G	5% (12/256)	39% (60/155)	24% (130/551)	8% (47/618)	27% (54/198)	26% (164/641)
PIK3C2G	p.K978N	3% (16/492)	45% (113/250)	23% (176/752)	10% (80/803)	22% (44/200)	28% (268/960)
GATA1	p.K315N	3% (5/192)	32% (35/111)	29% (313/1071)	14% (154/1067)	27% (100/370)	25% (419/1648)
EPHB1	p.I332M	2% (5/211)	26% (25/96)	26% (261/1015)	13% (120/919)	30% (102/343)	26% (348/1322)
ESR1	p.E380Q	2% (7/287)	68% (106/157)	46% (339/737)	19% (158/823)	58% (160/275)	53% (534/1009)
PAK7	p.E494*	2% (5/304)	38% (56/148)	28% (202/715)	12% (83/701)	25% (55/224)	30% (273/897)
MAP2K2	p.E207Q	NRD (2/137)	35% (40/113)	27% (221/815)	13% (106/823)	27% (72/270)	29% (309/1076)
FLT4	p.R282Q	NRD (2/89)	26% (12/47)	34% (225/667)	15% (98/638)	33% (89/270)	32% (266/820)

Table 2.1. Mutant allele fractions of somatic mutations identified in the primary breast tumour, liver metastasis and plasma samples. MAFs, mutant allele fractions. Color coding: dark gray

cells, MAF>50%; light gray cells, MAF 20-50%; pale gray cells, MAF 5-20%, and white cells, MAF<5% or no mutation identified (NRD, not reliably detected). Plasma 1, baseline; plasma 2, 2 months after initiation of AKT inhibitor Ipatasertib treatment; plasma 3, 6 months after initiation AKT inhibitor Ipatasertib treatment; plasma 4, at disease progression.

Evidence of tumour heterogeneity was observed, given that the liver metastasis was enriched for mutations either only present at low allele fractions in the primary tumour (i.e., <5% MAF; *PIK3C2G*, *GATA1*, *EPHB1*, *ESR1* and *PAK7*) or found at a MAF beyond the resolution obtained with the sequencing depth achieved for the primary tumour sample (i.e., FLT4 and MAP2K2 mutations)**(Table 2.1 and Figure 2.3)**.

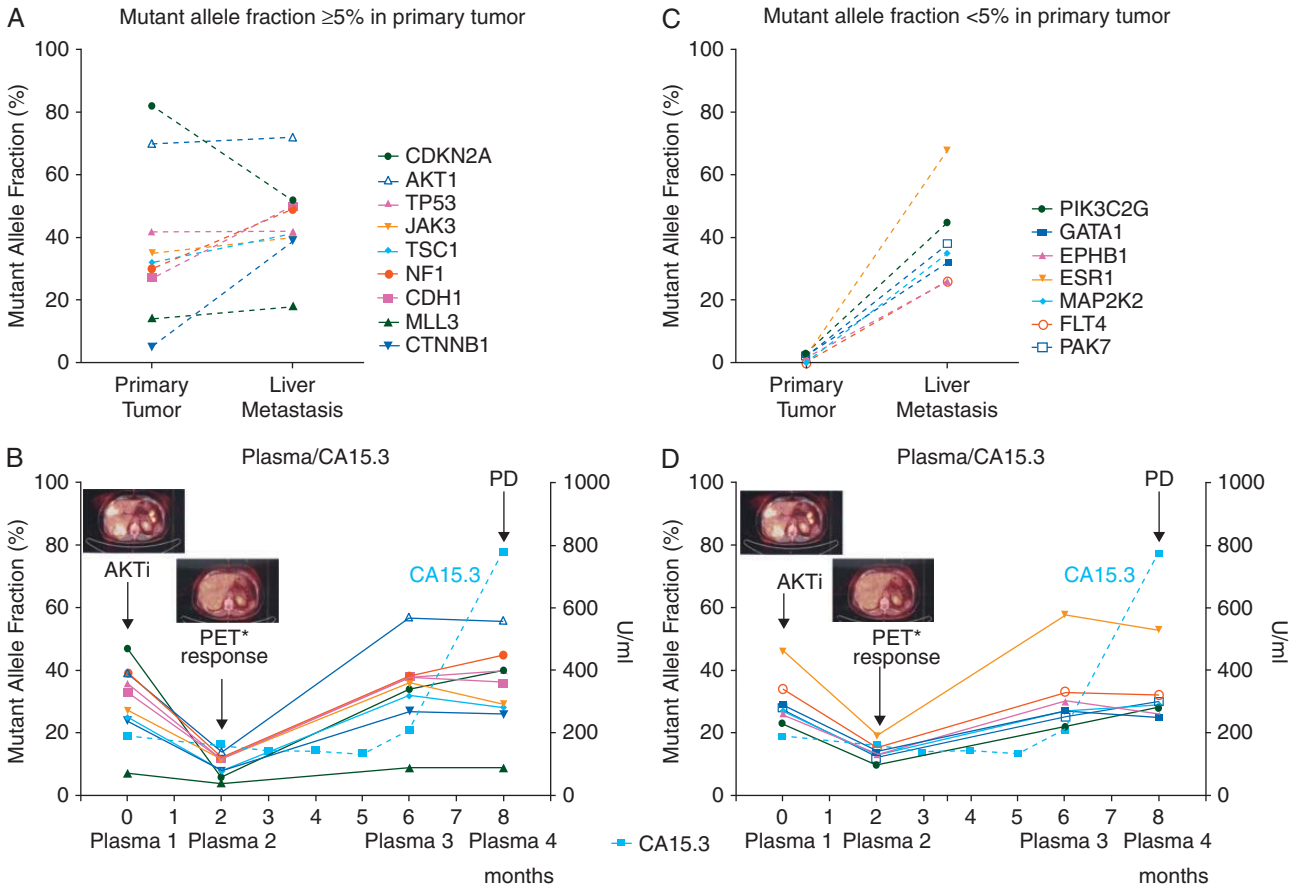

Figure 2.3. Identification of the mutant alleles in the primary tumour and metastasis in (A) and (C) and longitudinal monitoring of same mutant alleles in four plasma-derived ctDNA samples along with CA15.3 levels in (B) and (D). Genes whose high confidence mutations were detected at a mutant allele fraction (MAF) of ≥5% in the primary tumour are depicted in (A) and (B), whereas genes whose high confidence mutations were detected in the plasma-derived ctDNA,

but either absent or present at a MAF of <5% in the primary tumour, are illustrated in (C) and (D). In (B) and (D), representative PET–CT images obtained at baseline and 2 months after initiation of Ipatasertib monotherapy; CA15.3 levels assessed during the fourth line of systemic treatment with Ipatasertib monotherapy. Arrow, initiation of Ipatasertib (AKTi) monotherapy. PD, progressive disease; *PET–CT, pharmacodynamic response.

In the longitudinal monitoring of the patient, the mutant allele fractions identified in ctDNA samples varied over time and mirrored the pharmacodynamic response to the targeted therapy as assessed by positron emission tomography–computed tomography **(Figure 2.3).** Moreover, the increase in mutant alleles in plasma-derived ctDNA was observed before radiologic disease progression (data not shown), and before the increase in CA15.3 levels, providing evidence to suggest that increases in disease burden can be detected earlier by ctDNA analysis than by classical biochemical and radiologic assessments.

Discussion and conclusions

This proof-of-principle study demonstrates that high-depth targeted massively parallel sequencing of plasma-derived ctDNA constitutes a potential tool for *de novo* mutation identification and monitoring of somatic genomic alterations during the course of targeted therapy, and may be employed to overcome the challenges posed by intra-tumour genetic heterogeneity (10).

Breast and other cancers, at the time of diagnosis, have been shown be composed of heterogeneous populations of tumour cells that, in addition to the founder genetic events, harbour private mutations (43). Here we demonstrate that mutations affecting *ESR1*, *CTNNB1*, *PIK3C2G*, *GATA1*, *EPHB1*, *PAK7*, *MAP2K2* and *FLT4*, albeit present at allele fractions ≥26% in the metastatic lesion, were likely present in a minor clone of the primary tumour (i.e., MAFs ≤5%). Notably, in the present case all mutations detectable by targeted massively parallel sequencing of the metastatic lesion were also detected in the plasma ctDNA samples, showing that ctDNA may constitute an alternative to metastatic lesion sampling for targeted massively parallel sequencing analysis.

Activating *ESR1* mutations have been identified in endocrine-resistant metastatic lesions while not detectable in the respective primary breast cancers (44-46). In this study, the endocrine therapy resistance-associated *ESR1* E380Q mutation was present at a higher allele fraction in the ER-positive liver metastasis (MAF 68%) than in its synchronous ER-positive primary breast cancer (MAF 2%). Importantly, however, the biopsies of the synchronous primary

and metastatic lesions were collected before any systemic therapy. It remains to be determined whether the *ESR1* E380Q mutation provided a growth advantage at the metastatic site irrespective of treatment or merely co-segregated with other molecular alterations present in the clone that gave rise to the metastatic deposit.

A limitation of this work relies in the fact that the analyses were carried out utilizing DNA extracted from a single patient with a high disease burden and using targeted sequencing. The amounts of plasma DNA obtained from this patient were insufficient for whole genome or whole exome sequencing analysis at the depth that would be required to determine whether a specific genomic alteration would be selected by the administration of the targeted therapy, and to define whether there were mutations affecting genes not included in the MSK-IMPACT platform that would be present in the primary tumour and/or in the metastasis.

Although the longitudinal analysis of plasma ctDNA was valuable for disease monitoring, the analysis of the plasma DNA sample at progression did not result in the identification of a genetic aberration causative of resistance to Ipatasertib monotherapy. Although resistance to AKT inhibition may be mediated by adaptive changes (e.g. activation of up-stream receptor tyrosine kinases), it is unknown whether this mechanism would induce resistance to the Ipatasertib monotherapy in patients harboring AKT1 mutations.

In conclusion, high-depth targeted capture massively parallel sequencing analysis of plasma-derived circulating tumour DNA represents a potential tool to characterise the mutation repertoire of breast cancers and to monitor tumour burden and the somatic alterations in cancer cells during the course of targeted therapy.

Chapter 3: Cerebrospinal fluid-derived circulating tumour DNA better represents the genomic alterations of brain tumours than plasma

Introduction

The outcomes for patients with CNS malignancies remain poor. A growing understanding of the molecular features of GBM and brain metastasis from solid tumours has stimulated the discovery of biomarkers and the development of novel therapies, including the use of molecularly-based targeted agents (23, 30, 47-49).

There are several challenges and pitfalls while managing patients with CNS malignancies because of the lack of consistent biomarkers to assist in the diagnosis, serial monitoring and potential mechanisms of resistance to therapy (47). Therefore, many patients are subjected to invasive surgical procedures to determine disease status or experience treatment delays when radiographic imaging precludes accurate assessment of tumour response or progression (50).

The genomic characterisation and monitoring of brain malignancies is puzzling given the restricted sampling of tumours and the limited abundance of brain tumour-derived ctDNA in the plasma (12, 26, 27). In patients with primary brain tumours, the presence of ctDNA derived from plasma is minimal probably as a result of the blood-brain barrier. Analysis of an alternative body fluid which is in contact with the CNS malignant cells, the CSF, has shown evidence that nucleic acids, tumour cells, proteins, tumour-derived extracellular vesicles shed by cancer cells into the CSF to be a source of tumour-specific biomarkers (14, 25, 27-30, 33, 35, 51).

Because cell-free DNA from brain and spinal cord tumours cannot usually be reliably detected in the plasma, we hypothesised that CSF would serve as a liquid biopsy of brain malignancies by enabling measurement of ctDNA from CSF to characterise tumour-specific genomic alterations, monitor brain tumours over time and that ctDNA CSF would be superior to plasma (14) **(Figure 3.1)**.

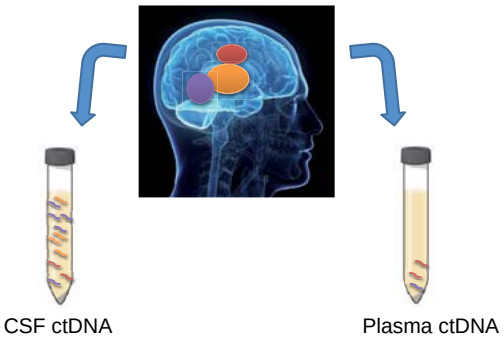

Figure 3.1. Schematics for comparison CSF ctDNA and plasma ctDNA.

Objectives

- Compare the collection of genetic alterations of the CSF ctDNA with that of plasma ctDNA in patients with primary and secondary CNS malignancies.
- Assess whether the analysis of CSF ctDNA could be useful for the characterisation of brain tumour 'private' somatic mutations.
- Assess whether the analysis of CSF ctDNA may serve for longitudinal monitoring of brain malignancies.
- Compare CSF ctDNA with cytopathologic analysis (leptomeningeal carcinomatosis, LC).

Results

Genomic characterisation of CSF ctDNA in brain malignancies

Hybridization capture-based massively parallel targeted sequencing **(Appendices Supplementary Data 1)** and/or exome sequencing coupled with droplet digital PCR (ddPCR) was applied to synchronous CSF and plasma-derived ctDNA, and tumour tissue deposits from the patients with GBM, medulloblastoma (Medullo), and brain metastases from lung cancer (BMLC) and from breast cancer (BMBC, six of them subjected to warm autopsies) including breast cancer patients with clinical features suggestive of LC.

In all cases, except BMBCs, CSF was obtained at the same time as plasma through lumbar puncture or cerebral shunts normally obtaining 1-2 ml of CSF. Tumours and fluids from all 6 cases of BMBCs were obtained through warm autopsy and the CSF was collected from the cisterna magna.

CSF ctDNA performs better than plasma ctDNA

In order to study and compare the ctDNA present in the CSF with plasma ctDNA, we sequenced DNA obtained from tumour samples, germline DNA (peripheral blood lymphocytes), plasma and CSF of a cohort of 12 patients (4 GBM, 6 BMBCs, 2 BMLCs) **(Appendices Table A1)**. Patients were divided into two groups depending on the amount of extracranial tumour burden **(Appendices Table A2)**. **Figure 3.2** shows the representation of the non-silent genetic alterations from each of the twelve cases (i.e., patients with restricted CNS disease and patients with disseminated disease - CNS and non-CNS disease) and phylogenetic trees of the autopsied patients with brain metastasis from breast cancer are represented.

In all cases, somatic single nucleotide variants (SNVs), insertion/deletions (indels) and copy number alterations (CNA) were identified in CSF ctDNA and plasma ctDNA, and validated in the brain tumour tissue from the respective patients **(Figures 3.2 and 3.3)**

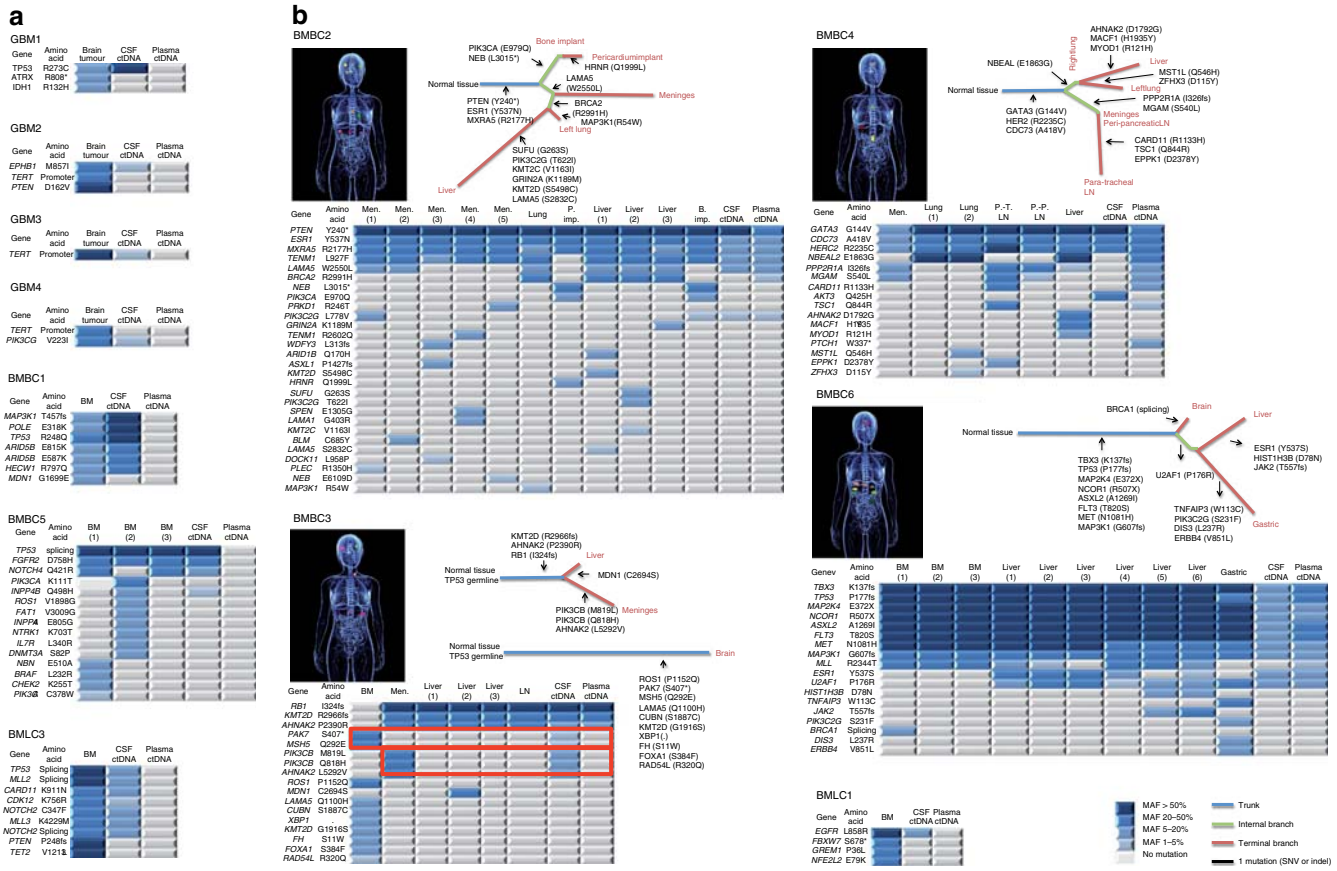

Figure 3.2. CSF ctDNA better captures the genomic alterations in patients with brain tumours than plasma ctDNA. (a,b) Analysis of CSF ctDNA, plasma ctDNA and primary brain tumour or metastatic lesions collected simultaneously. Heatmap of the non-silent genetic alterations from each of the twelve cases is shown and phylogenetic trees of the autopsied patients with brain metastasis from breast cancer (BMBC) are represented. Colour key for mutant allelic frequencies (MAFs) is shown. (a) Patients with restricted central nervous system (CNS) disease, glioblastoma (GBM), BMBC and brain metastasis from lung cancer (BMLC). (b) Patients with CNS and non-CNS disease. BM, brain metastasis; LN, lymph node; Men, meninges; P. Imp, pericardium implant; PT, para-tracheal; PP, peri-pancreatic.

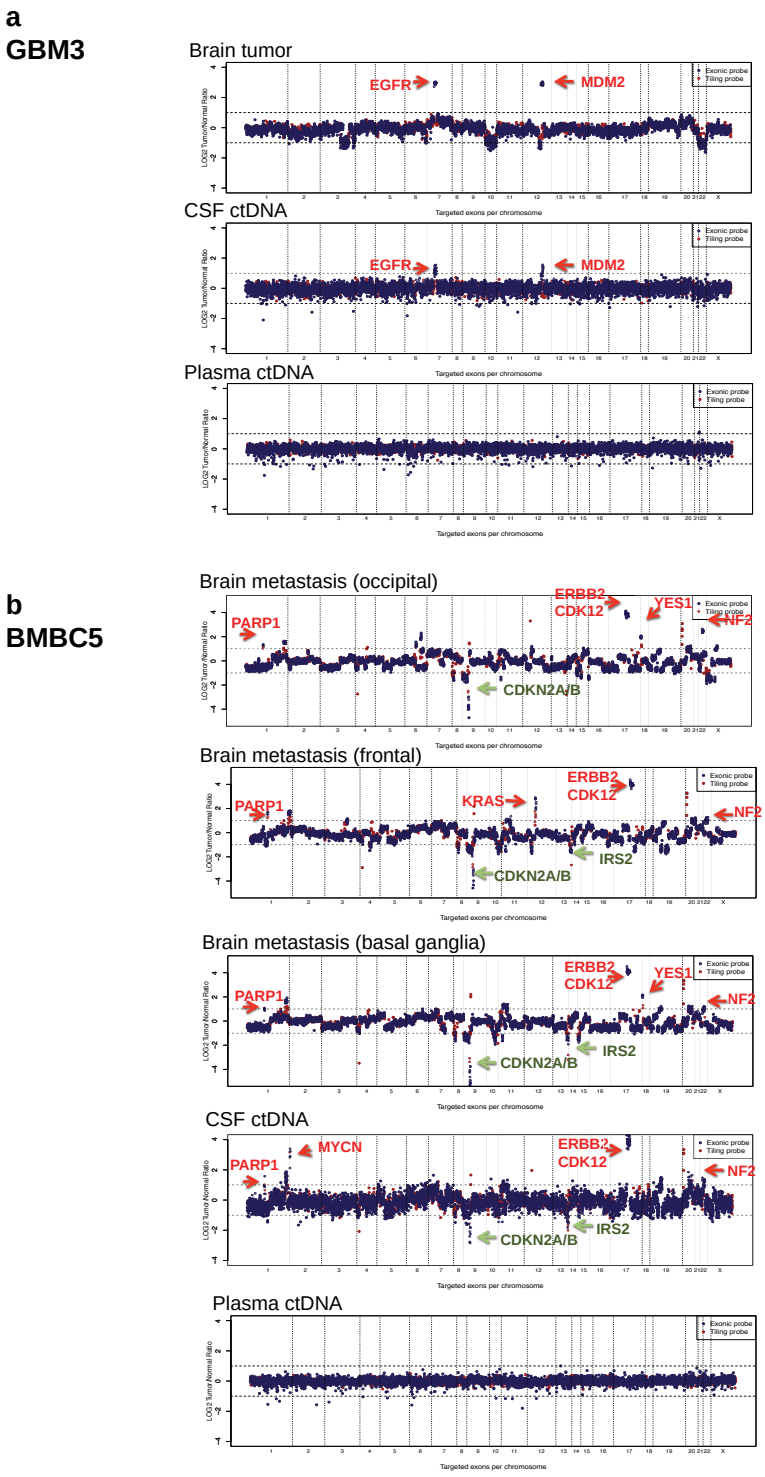

Figure 3.3. Gene copy number alterations across the brain tumour, CSF, plasma which were collected simultaneously in (a) a patient with glioblastoma (b) a patient with brain metastasis from breast cancer (BMBC). Note that plasma ctDNA did not play a role in such patients with minimal or absent CNS disease.

In addition, we sequenced the DNA concomitantly extracted from the CSF and plasma in an expansion cohort of 11 patients (2 Medullos, 5 BMLCs, 4 BMBCs) with CNS restricted disease and barely any visceral tumour burden in order to facilitate the comparison of the contribution of the brain tumour DNA into the CSF or plasma ctDNA **(Figure 3.4, Appendices Table A3)**. In all cases, CSF ctDNA was detected and harboured gene mutations that were either absent or detected with lower MAFs in plasma ctDNA.

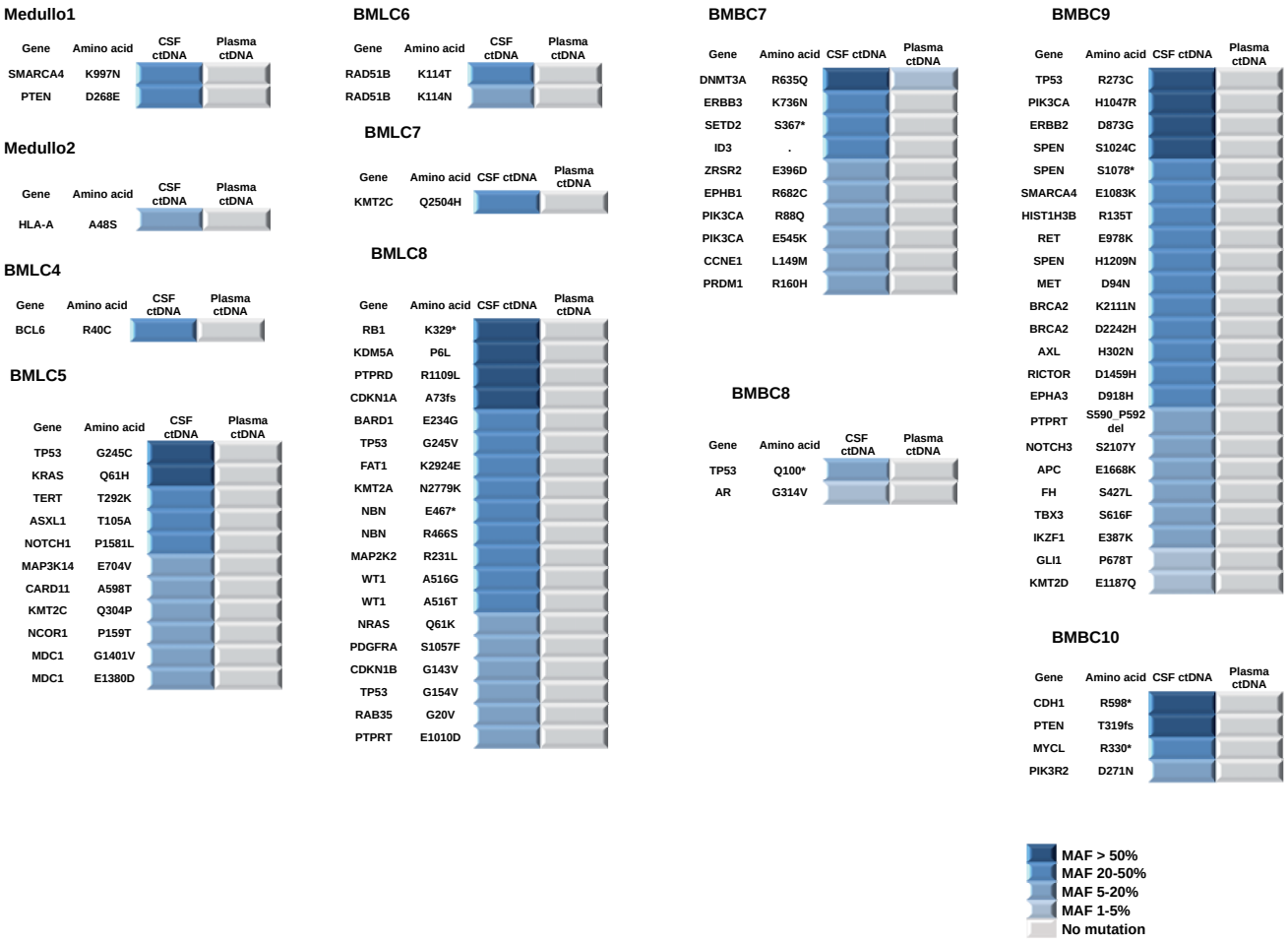

Figure 3.4. Expansion cohort comparing CSF ctDNA and plasma ctDNA collected simultaneously in patients with brain tumours. Heatmap of the non-silent genetic alterations from each of the cases is shown. Colour key for mutant allelic frequencies (MAFs) is represented.

Our experiments confirmed that ctDNA-derived from the CSF characterised the genomic alterations of CNS disease better than plasma in both primary and secondary brain tumours (14) **(Figures 3.2, 3.3, 3.4)**.

In a subset analysis of a breast cancer autopsies series, patients with CNS restricted disease (i.e., minimal or absent extra-cranial disease), the mutations present in brain metastasis were captured by ctDNA in CSF and not in plasma. By contrast, in patients with abundant visceral disease, tumour-derived mutations in the CSF and plasma ctDNA were comparable.

In the case of samples from the autopsy material of patients BMBC2, BMBC3, BMBC4 and BMBC6, we had enough number of specimens to infer phylogenetic trees representing the genomic subclonal diversity and be able to identify trunk ubiquitous genetic mutations. Interestingly, trunk mutations were always identified in the CSF ctDNA **(Figure 3.2).**

Notably, CSF-derived ctDNA identified CNS-specific private mutations (i.e. brain and meningeal private mutations) in a patient with Li Fraumeni syndrome and concurrent two neoplasms (i.e., HER2-positive metastatic breast cancer and esthesioneuroblastoma) **(Figure 3.2b and Figure 3.5)**. The patient displayed two sets of tumours: the breast cancer-derived brain metastasis and, independently, the meningeal implants and liver metastases **(Figure 3.5)**. The mutations of the brain metastasis were not present in the extracranial tumours and, moreover, three private gene mutations (*PIK3CB* M819L, *PIK3CB* Q818H, *AHNAK2* L5292V) were exclusively present in the meningeal lesion **(Figure 3.2b – see boxed mutations)**. The gene mutations with the highest MAFs of the brain metastasis and the private mutations in the meningeal lesions were present in the CSF ctDNA and not in the plasma ctDNA indicating that brain private mutations are more represented in the ctDNA from CSF than plasma.

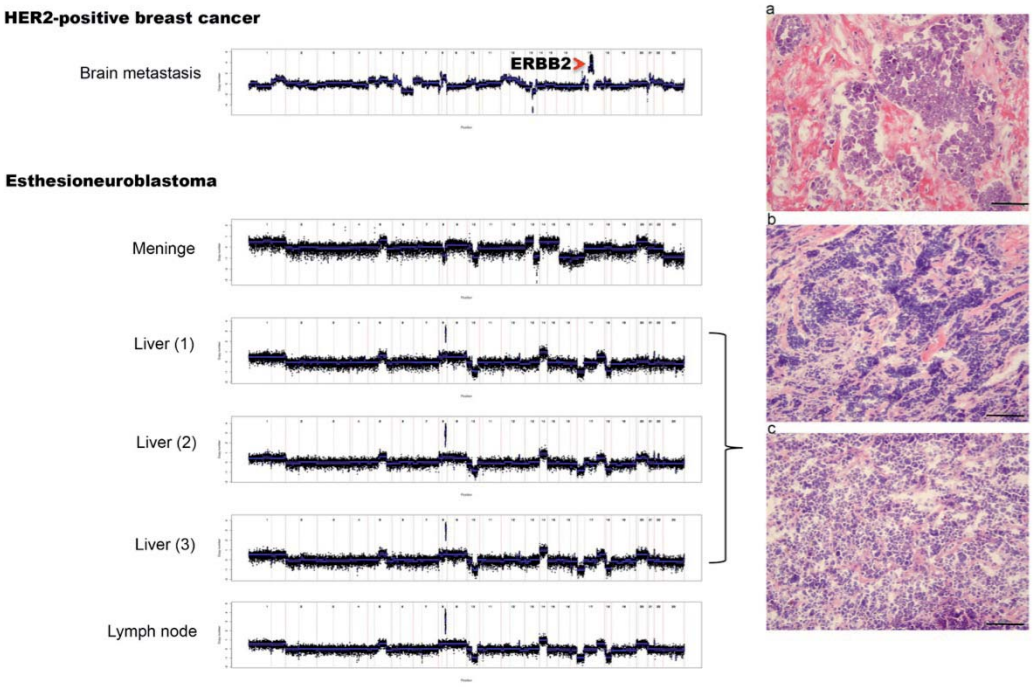

Figure 3.5. Genomic analysis of a patient with Li Fraumeni syndrome and a diagnosis of both HER2-positive metastatic breast cancer and esthesioneuroblastoma (BMBC3). The brain metastasis was inferred to be originated from the HER2-positive metastatic breast cancer, as *ERBB2* gene copy amplification is shown at the genomic position 17q12. Micrographs representing (a) brain metastasis; (b) meninges; (c) liver metastasis. Scale bar = 500 μm

Sensitivity analysis of CSF ctDNA and plasma ctDNA

In patients with a CNS restricted disease, the MAFs in all samples of CSF ctDNA were significantly higher than in plasma **(Figure 3.6)**. The sensitivity for somatic mutations of the CNS was significantly higher in CSF ctDNA than plasma ctDNA **(Figure 3.7, Appendices Table A4)**.

It should be noted, however that some mutations were detected in the CSF or plasma but not in the brain tumour specimen **(Figure 3.2)**. These could be potential false positives or mutations not present in the sequenced tumour fragment but present in another region of the brain tumour. In patients with abundant visceral disease **(Figure 3.2)**, the MAFs of the gene mutations in the CSF and plasma ctDNA were comparable.

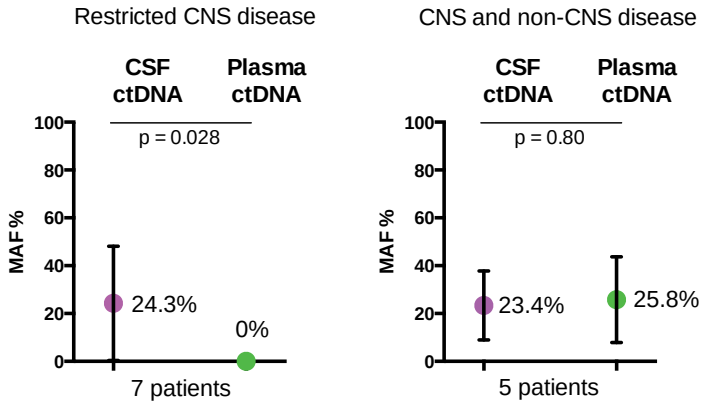

Figure 3.6. Comparison of the mutant allelic frequencies (MAF) of CSF ctDNA and plasma ctDNA in CNS restricted disease and CNS and non-CNS disease. Data were pooled and the mean with SD error bars is shown (Mann-Whitney test).

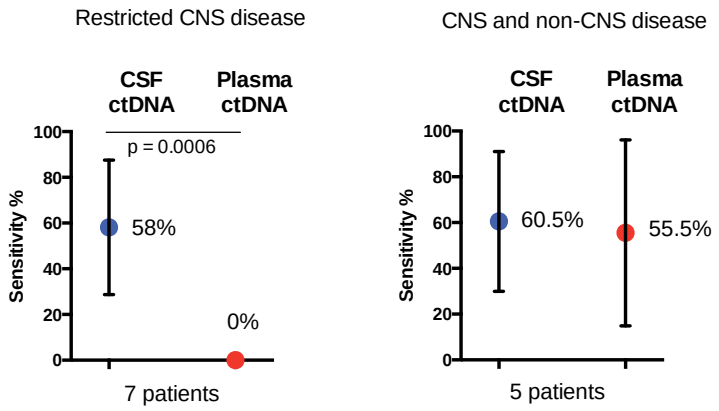

Figure 3.7. Sensitivity analysis of CSF ctDNA and plasma ctDNA. Sensitivity was inferred based on gene mutations detected in central nervous system (CNS) tumours, which were either identified in CSF or plasma ctDNA. Data were pooled and the mean with standard deviation error bars is shown. A Mann–Whitney test was used for the analysis and P value is shown.

Longitudinally monitoring of primary brain tumours and brain metastasis with CSF ctDNA

Concomitantly CSF and plasma were obtained from six patients (GBM and metastatic breast and lung cancer patients with brain metastasis and minimal or absent extracranial disease) at sequential time points **(Figure 3.8)**.

Brain lesions were identified using magnetic resonance imaging (MRI) and brain tumour burden was quantified using computer aided planimetric analysis **(Appendices Table A5)**. The tumour somatic genomic alterations, previously identified in the tumours by exome sequencing, were determined in the CSF-derived DNA of the patients through ddPCR. The MAFs in all samples of CSF ctDNA were higher than in plasma **(Appendices Table A6)**, were modulated over time and followed the same trend as the variation in brain tumour burden.

MAFs of CSF ctDNA decreased with surgical resection and/or responses to systemic therapy and increased with tumour progression, showing that the amount of ctDNA present in the CSF fluctuates with time and may be representative of the brain tumour progression.

For instance, patient GBM3 is 64 year-old woman with diagnosis of temporal glioblastoma (IDH1 negative, *EGFR* mutant) **(Figure 3.8)**. She was subjected to partial resection of the brain tumour. Then, she was treated with a targeted therapy plus temozolomide, concomitantly with whole brain radiotherapy. The mutations *EGFR* R108K, *FTH1* I146T, *OR51D1* R135C targeted in the body fluids (i.e., CSF and plasma) by ddPCR were substantially enriched in CSF ctDNA as compared to plasma and dropped after surgical resection, reflecting the findings of the MRI of the brain.

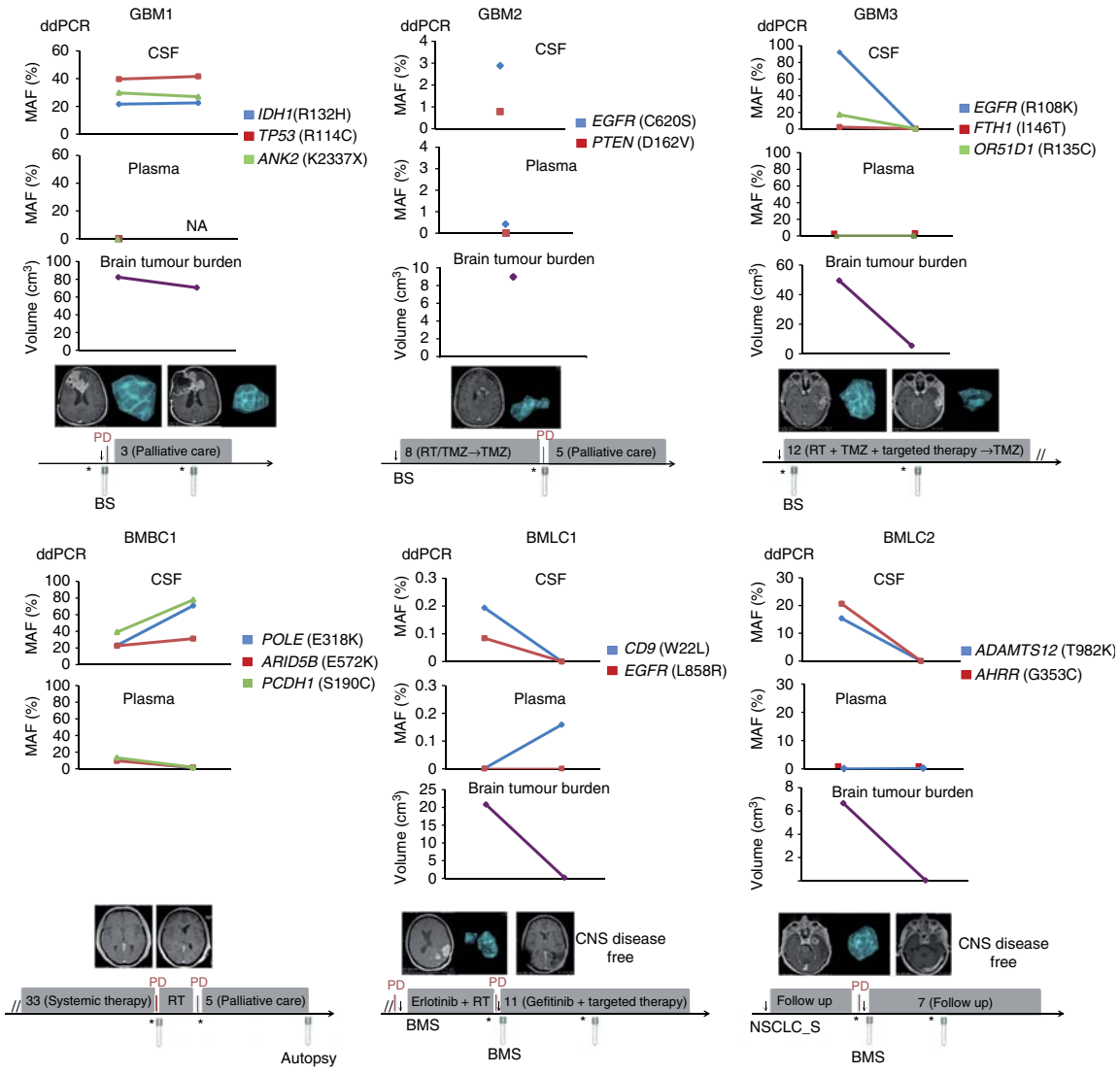

Figure 3.8. Dynamic changes in CSF ctDNA recapitulate the treatment courses of patients with brain tumours. Longitudinal monitoring of patients with GBM and brain metastases through CSF and plasma ctDNA and the analysis of brain tumour burden. Gene mutations were measured by ddPCR. Tumour volumes were calculated using computer aided planimetric analysis. Timelines reflect the most relevant clinical information for each patient. BS, brain surgery; BMS, brain metastasis surgery; CNS, central nervous system; NSCLC_S, non-small cell lung cancer surgery; PD, progressive disease; RT, radiotherapy; TMZ, temozolomide. Asterisk and arrow indicate time of magnetic resonance imaging and surgical procedure, respectively. Grey boxes indicate therapy or follow up, and their duration is provided in months.

CSF ctDNA complements the diagnosis of leptomeningeal carcinomatosis

Leptomeningeal carcinomatosis (LC) represents a rare but often dreadful complication of advanced cancers. It refers to the multifocal seeding of the leptomeninges by malignant cells.

Signs and symptoms such as headache, nuchal rigidity, motor weakness, cranial nerve palsies and photophobia indicates meninges involvement and should lead to rapid work-up and treatment. LC diagnosis relies on clinical symptomatology, detection of malignant cells in the CSF by CSF cytology (spinal tap) and MRI. Diagnosis of LC is not trivial and its misdiagnosis has important clinical implications. The treatment goal is to improve the neurological status of the patient and to prolong survival.

The identification of CSF ctDNA led to the hypothesis that cell-free DNA in the CSF could be used as a diagnostic tool for LC. To define whether the analysis of CSF ctDNA can be employed to enhance the sensitivity of the detection of LC by cytopathologic analysis of CSF, standard of care cytopathologic analysis was performed and CSF ctDNA sequencing in the same samples obtained from three breast cancer patients with clinical signs and symptoms suggestive of LC.

Importantly, there were divergences between the cytology and the CSF ctDNA analyses **(Figure 3.9)**.

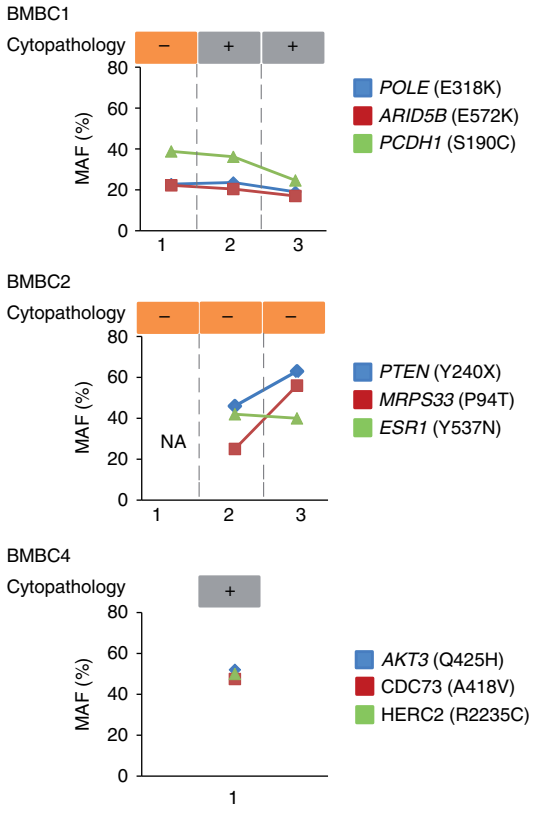

Figure 3.9. Analysis of CSF ctDNA as a diagnostic tool for LC in 3 metastatic breast cancer patients. The results of serial clinical cytopathology analyses are shown in the upper part of the graph. In the lower part, mutant allelic frequencies (MAFs) measured by ddPCR in the same CSF samples are depicted. NA, not available.

In BMBC2, although three cytopathologic analyses yielded negative results, MAFs ranging from 20 to 50% in the two CSF samples were detected in the samples that were available. Given that LC was confirmed at the autopsy of BMBC2, the results indicated that the CSF ctDNA analysis detected disease at a level not detectable by cytopathologic analysis.

In BMBC1, one of the cytopathologic analysis was discordant with the presence of CSF ctDNA while in BMBC4 the results of the cytopathologic analysis and the CSF ctDNA were in agreement. In both cases, BMBC1 and BMBC4, LC was confirmed at the autopsy.

Discussion and conclusions

In this study (14), we identified and characterised ctDNA in the CSF of patients with brain malignancies and compared it to plasma ctDNA. We showed that CSF ctDNA is more representative of brain tumour genomic alterations than plasma and putative actionable gene mutations and CNA (i.e. *EGFR*, *PTEN*, *ESR1, IDH1, ERBB2, FGFR2*) can be identified and monitored.

CSF ctDNA has a significantly higher sensitivity than plasma for CNS genomic alterations and can be used to detect brain tumour private mutations and to monitor brain tumour progression and response to treatment. In addition, CSF may be a useful biomarker to complement the diagnosis of LC.

GBM is a dreadful condition characterised by predictable tumour relapse. Notably, relapsed tumours tend to evolve under selective pressures (i.e., therapy) and present different genomic alterations than the primary tumour (52). Surgical procedures (resection and biopsies) are seldom indicated in relapsed GBM limiting its genomic characterisation and precluding the treatment of the relapsed GBM based on genomic information. CSF ctDNA provides a minimally invasive method to assess the genomic alterations of the relapsed tumour helping to select the optimal treatment dictated by the molecular characteristics of the brain cancer.

Patients with brain metastasis also exhibit a dismal prognosis and are usually recalcitrant to treatments. Recent evidence show that clinically actionable alterations present in brain metastases are frequently not detected in primary biopsies, suggesting that sequencing of primary biopsies alone or other systemic metastasis may miss a substantial number of opportunities for targeted therapy (48, 53-55). The identification and monitoring of the brain metastasis' specific genomic alterations through CSF ctDNA may expedite the design of tailored treatments to target brain metastasis.

Patients that have LC have dismal outcomes and have lack of effective therapeutic options. Our results pave the way to the possibility of using CSF ctDNA to complement the

diagnosis of LC. The identification of the molecular makeup of each patient is critical in tackling cancer with greater precision. Further studies with a higher number of patients will be needed to consolidate this methodology for the diagnosis and longitudinal monitoring of patients with LC.

In summary, these results build a proof-of-concept that opens the possibility to use CSF ctDNA in the management of patients with brain malignancies.

Chapter 4: Final Conclusions

The genomic characterisation of cancers to guide treatment assessments is progressively being applied in medical oncology clinical care and in clinical trials. However, these genomic analyses, including mutation and copy number alterations, are typically performed on tumour tissue biopsies acquired at diagnosis and are subjected to sample availability and sampling bias due to tumour heterogeneity. The personalisation of cancer treatments have adopted the so-called 'liquid biopsies', particularly cell-free ctDNA detected in plasma and body fluids as tools to non-invasively scan tumour genomes, quantify tumour burden, and monitor systemic therapies to identify therapy resistance.

The ancillary article presented "**Capturing intra-tumour genetic heterogeneity by de novo mutation profiling of circulating cell-free tumour DNA: a proof-of-principle" (10)** published in *Annals of Oncology* in 2014**,** shows that plasma-derived ctDNA can be exploited as a liquid biopsy for patients with metastatic breast cancers and high tumour burden. The inter-metastatic heterogeneity (i.e., mutation repertoire of a primary tumour and a synchronous metastasis) and the modulation of these mutations during the course of targeted therapy can be uncovered using plasma ctDNA. These results can be applicable in other scenarios and cancer types, considering the sequencing technology has sufficient sensitivity and specificity for capturing mutations in plasma ctDNA. Therefore, ctDNA constitutes a potential surrogate for tumour DNA obtained from tissue biopsies, also provides a means for longitudinal analysis of tumour genomes, and may be employed to understand tumour heterogeneity.

The main article presented **"Cerebrospinal fluid-derived circulating tumour DNA better represents the genomic alterations of brain tumours than plasma" (14)** published in *Nature Communications* in November 2015 shows that the analysis of CSF ctDNA is superior in terms of genomic characterisation and monitoring of CNS malignancies in comparison to plasma ctDNA. The results indicate that CSF ctDNA can be exploited as a liquid biopsy for brain malignancies and can open new research avenues to establish these biomarkers as non-invasive tools for the genomic characterisation, diagnosis, serial monitoring and determining outcomes without the need of invasive procedures.

Taken together, ctDNA present in the CSF for brain malignancies and ctDNA present in the plasma for breast cancers with extra-cranial systemic metastases may be used to characterise metastasis-specific genomic alterations providing information to adapt the therapeutic management of patients.

References

1. Bedard PL, Hansen AR, Ratain MJ, Siu LL. Tumour heterogeneity in the clinic. Nature. 2013;501:355-64.

2. De Mattos-Arruda L, Caldas C. Cell-free circulating tumour DNA as a liquid biopsy in breast cancer. Molecular oncology. 2015.

3. Haber DA, Velculescu VE. Blood-based analyses of cancer: circulating tumor cells and circulating tumor DNA. Cancer discovery. 2014;4:650-61.

4. De Mattos-Arruda L, Cortes J, Santarpia L, Vivancos A, Tabernero J, Reis-Filho JS, Seoane J. Circulating tumour cells and cell-free DNA as tools for managing breast cancer. Nature reviews Clinical oncology. 2013;10:377-89.

5. Leary RJ, Kinde I, Diehl F, Schmidt K, Clouser C, Duncan C, Antipova A, Lee C, McKernan K, De La Vega FM, Kinzler KW, Vogelstein B, Diaz LA, Jr., Velculescu VE. Development of personalized tumor biomarkers using massively parallel sequencing. Science translational medicine. 2010;2:20ra14.

6. Leary RJ, Sausen M, Kinde I, Papadopoulos N, Carpten JD, Craig D, O'Shaughnessy J, Kinzler KW, Parmigiani G, Vogelstein B, Diaz LA, Jr., Velculescu VE. Detection of chromosomal alterations in the circulation of cancer patients with whole-genome sequencing. Science translational medicine. 2012;4:162ra54.

7. Forshew T, Murtaza M, Parkinson C, Gale D, Tsui DW, Kaper F, Dawson SJ, Piskorz AM, Jimenez-Linan M, Bentley D, Hadfield J, May AP, Caldas C, Brenton JD, Rosenfeld N. Noninvasive identification and monitoring of cancer mutations by targeted deep sequencing of plasma DNA. Science translational medicine. 2012;4:136ra68.

8. Murtaza M, Dawson SJ, Tsui DW, Gale D, Forshew T, Piskorz AM, Parkinson C, Chin SF, Kingsbury Z, Wong AS, Marass F, Humphray S, Hadfield J, Bentley D, Chin TM, Brenton JD, Caldas C, Rosenfeld N. Non-invasive analysis of acquired resistance to cancer therapy by sequencing of plasma DNA. Nature. 2013;497:108-12.

9. Dawson SJ, Tsui DW, Murtaza M, Biggs H, Rueda OM, Chin SF, Dunning MJ, Gale D, Forshew T, Mahler-Araujo B, Rajan S, Humphray S, Becq J, Halsall D, Wallis M, Bentley D, Caldas C, Rosenfeld N. Analysis of circulating tumor DNA to monitor metastatic breast cancer. The New England journal of medicine. 2013;368:1199-209.

10. De Mattos-Arruda L, Weigelt B, Cortes J, Won HH, Ng CK, Nuciforo P, Bidard FC, Aura C, Saura C, Peg V, Piscuoglio S, Oliveira M, Smolders Y, Patel P, Norton L, Tabernero J, Berger MF, Seoane J, Reis-Filho JS. Capturing intra-tumor genetic heterogeneity by de novo

mutation profiling of circulating cell-free tumor DNA: a proof-of-principle. Annals of oncology : official journal of the European Society for Medical Oncology / ESMO. 2014;25:1729-35.

11. Rothe F, Laes JF, Lambrechts D, Smeets D, Vincent D, Maetens M, Fumagalli D, Michiels S, Drisis S, Moerman C, Detiffe JP, Larsimont D, Awada A, Piccart M, Sotiriou C, Ignatiadis M. Plasma circulating tumor DNA as an alternative to metastatic biopsies for mutational analysis in breast cancer. Annals of oncology : official journal of the European Society for Medical Oncology / ESMO. 2014;25:1959-65.

12. Bettegowda C, Sausen M, Leary RJ, Kinde I, Wang Y, Agrawal N, Bartlett BR, Wang H, Luber B, Alani RM, Antonarakis ES, Azad NS, Bardelli A, Brem H, Cameron JL, Lee CC, Fecher LA, Gallia GL, Gibbs P, Le D, Giuntoli RL, Goggins M, Hogarty MD, Holdhoff M, Hong SM, Jiao Y, Juhl HH, Kim JJ, Siravegna G, Laheru DA, Lauricella C, Lim M, Lipson EJ, Marie SK, Netto GJ, Oliner KS, Olivi A, Olsson L, Riggins GJ, Sartore-Bianchi A, Schmidt K, Shih I M, Oba-Shinjo SM, Siena S, Theodorescu D, Tie J, Harkins TT, Veronese S, Wang TL, Weingart JD, Wolfgang CL, Wood LD, Xing D, Hruban RH, Wu J, Allen PJ, Schmidt CM, Choti MA, Velculescu VE, Kinzler KW, Vogelstein B, Papadopoulos N, Diaz LA, Jr. Detection of circulating tumor DNA in early- and late-stage human malignancies. Science translational medicine. 2014;6:224ra24.

13. Olsson E, Winter C, George A, Chen Y, Howlin J, Tang MH, Dahlgren M, Schulz R, Grabau D, van Westen D, Ferno M, Ingvar C, Rose C, Bendahl PO, Ryden L, Borg A, Gruvberger-Saal SK, Jernstrom H, Saal LH. Serial monitoring of circulating tumor DNA in patients with primary breast cancer for detection of occult metastatic disease. EMBO molecular medicine. 2015.

14. De Mattos-Arruda L, Mayor R, Ng CK, Weigelt B, Martinez-Ricarte F, Torrejon D, Oliveira M, Arias A, Raventos C, Tang J, Guerini-Rocco E, Martinez-Saez E, Lois S, Marin O, de la Cruz X, Piscuoglio S, Towers R, Vivancos A, Peg V, Ramon y Cajal S, Carles J, Rodon J, Gonzalez-Cao M, Tabernero J, Felip E, Sahuquillo J, Berger MF, Cortes J, Reis-Filho JS, Seoane J. Cerebrospinal fluid-derived circulating tumour DNA better represents the genomic alterations of brain tumours than plasma. Nature communications. 2015;6:8839.

15. Murtaza M, Dawson SJ, Pogrebniak K, Rueda OM, Provenzano E, Grant J, Chin SF, Tsui DW, Marass F, Gale D, Ali HR, Shah P, Contente-Cuomo T, Farahani H, Shumansky K, Kingsbury Z, Humphray S, Bentley D, Shah SP, Wallis M, Rosenfeld N, Caldas C. Multifocal clonal evolution characterized using circulating tumour DNA in a case of metastatic breast cancer. Nature communications. 2015;6:8760.

16. Newman AM, Bratman SV, To J, Wynne JF, Eclov NC, Modlin LA, Liu CL, Neal JW, Wakelee HA, Merritt RE, Shrager JB, Loo BW, Jr., Alizadeh AA, Diehn M. An ultrasensitive method for quantitating circulating tumor DNA with broad patient coverage. Nature medicine. 2014;20:548-54.

17. Siravegna G, Mussolin B, Buscarino M, Corti G, Cassingena A, Crisafulli G, Ponzetti A, Cremolini C, Amatu A, Lauricella C, Lamba S, Hobor S, Avallone A, Valtorta E, Rospo G, Medico E, Motta V, Antoniotti C, Tatangelo F, Bellosillo B, Veronese S, Budillon A, Montagut C, Racca P, Marsoni S, Falcone A, Corcoran RB, Di Nicolantonio F, Loupakis F, Siena S, Sartore-Bianchi A, Bardelli A. Clonal evolution and resistance to EGFR blockade in the blood of colorectal cancer patients. Nature medicine. 2015;21:827.

18. Mouliere F, Rosenfeld N. Circulating tumor-derived DNA is shorter than somatic DNA in plasma. Proceedings of the National Academy of Sciences of the United States of America. 2015;112:3178-9.

19. Jahr S, Hentze H, Englisch S, Hardt D, Fackelmayer FO, Hesch RD, Knippers R. DNA fragments in the blood plasma of cancer patients: quantitations and evidence for their origin from apoptotic and necrotic cells. Cancer research. 2001;61:1659-65.

20. Diaz LA, Jr., Bardelli A. Liquid biopsies: genotyping circulating tumor DNA. Journal of clinical oncology : official journal of the American Society of Clinical Oncology. 2014;32:579-86.

21. Omuro A, DeAngelis LM. Glioblastoma and other malignant gliomas: a clinical review. Jama. 2013;310:1842-50.

22. Stelzer KJ. Epidemiology and prognosis of brain metastases. Surgical neurology international. 2013;4:S192-202.

23. Seoane J, De Mattos-Arruda L. Brain metastasis: new opportunities to tackle therapeutic resistance. Molecular oncology. 2014;8:1120-31.

24. Sottoriva A, Spiteri I, Piccirillo SG, Touloumis A, Collins VP, Marioni JC, Curtis C, Watts C, Tavare S. Intratumor heterogeneity in human glioblastoma reflects cancer evolutionary dynamics. Proceedings of the National Academy of Sciences of the United States of America. 2013;110:4009-14.

25. Best MG, Sol N, Zijl S, Reijneveld JC, Wesseling P, Wurdinger T. Liquid biopsies in patients with diffuse glioma. Acta neuropathologica. 2015;129:849-65.

26. Lavon I, Refael M, Zelikovitch B, Shalom E, Siegal T. Serum DNA can define tumor-specific genetic and epigenetic markers in gliomas of various grades. Neuro-oncology. 2010;12:173-80.

27. Chen WW, Balaj L, Liau LM, Samuels ML, Kotsopoulos SK, Maguire CA, Loguidice L, Soto H, Garrett M, Zhu LD, Sivaraman S, Chen C, Wong ET, Carter BS, Hochberg FH, Breakefield XO, Skog J. BEAMing and Droplet Digital PCR Analysis of Mutant IDH1 mRNA in Glioma Patient Serum and Cerebrospinal Fluid Extracellular Vesicles. Molecular therapy Nucleic acids. 2013;2:e109.

28. Muller C, Holtschmidt J, Auer M, Heitzer E, Lamszus K, Schulte A, Matschke J, Langer-Freitag S, Gasch C, Stoupiec M, Mauermann O, Peine S, Glatzel M, Speicher MR, Geigl JB, Westphal M, Pantel K, Riethdorf S. Hematogenous dissemination of glioblastoma multiforme. Science translational medicine. 2014;6:247ra101.

29. Sullivan JP, Nahed BV, Madden MW, Oliveira SM, Springer S, Bhere D, Chi AS, Wakimoto H, Rothenberg SM, Sequist LV, Kapur R, Shah K, Iafrate AJ, Curry WT, Loeffler JS, Batchelor TT, Louis DN, Toner M, Maheswaran S, Haber DA. Brain tumor cells in circulation are enriched for mesenchymal gene expression. Cancer discovery. 2014;4:1299-309.

30. Seoane J, De Mattos-Arruda L. Escaping out of the brain. Cancer discovery. 2014;4:1259-61.

31. Segal MB. Extracellular and cerebrospinal fluids. Journal of inherited metabolic disease. 1993;16:617-38.

32. Rhodes CH, Honsinger C, Sorenson GD. Detection of tumor-derived DNA in cerebrospinal fluid. Journal of neuropathology and experimental neurology. 1994;53:364-8.

33. Pan W, Gu W, Nagpal S, Gephart MH, Quake SR. Brain tumor mutations detected in cerebral spinal fluid. Clinical chemistry. 2015;61:514-22.

34. Yang H, Cai L, Zhang Y, Tan H, Deng Q, Zhao M, Xu X. Sensitive detection of EGFR mutations in cerebrospinal fluid from lung adenocarcinoma patients with brain metastases. The Journal of molecular diagnostics : JMD. 2014;16:558-63.

35. Wang Y, Springer S, Zhang M, McMahon KW, Kinde I, Dobbyn L, Ptak J, Brem H, Chaichana K, Gallia GL, Gokaslan ZL, Groves ML, Jallo GI, Lim M, Olivi A, Quinones-Hinojosa A, Rigamonti D, Riggins GJ, Sciubba DM, Weingart JD, Wolinsky JP, Ye X, Oba-Shinjo SM, Marie SK, Holdhoff M, Agrawal N, Diaz LA, Jr., Papadopoulos N, Kinzler KW, Vogelstein B, Bettegowda C. Detection of tumor-derived DNA in cerebrospinal fluid of patients with primary tumors of the brain and spinal cord. Proceedings of the National Academy of Sciences of the United States of America. 2015;112:9704-9.

36. Gerlinger M, Rowan AJ, Horswell S, Larkin J, Endesfelder D, Gronroos E, Martinez P, Matthews N, Stewart A, Tarpey P, Varela I, Phillimore B, Begum S, McDonald NQ, Butler A, Jones D, Raine K, Latimer C, Santos CR, Nohadani M, Eklund AC, Spencer-Dene B, Clark G,

Pickering L, Stamp G, Gore M, Szallasi Z, Downward J, Futreal PA, Swanton C. Intratumor heterogeneity and branched evolution revealed by multiregion sequencing. The New England journal of medicine. 2012;366:883-92.

37. Aparicio S, Caldas C. The implications of clonal genome evolution for cancer medicine. The New England journal of medicine. 2013;368:842-51.

38. Yates LR, Gerstung M, Knappskog S, Desmedt C, Gundem G, Van Loo P, Aas T, Alexandrov LB, Larsimont D, Davies H, Li Y, Ju YS, Ramakrishna M, Haugland HK, Lilleng PK, Nik-Zainal S, McLaren S, Butler A, Martin S, Glodzik D, Menzies A, Raine K, Hinton J, Jones D, Mudie LJ, Jiang B, Vincent D, Greene-Colozzi A, Adnet PY, Fatima A, Maetens M, Ignatiadis M, Stratton MR, Sotiriou C, Richardson AL, Lonning PE, Wedge DC, Campbell PJ. Subclonal diversification of primary breast cancer revealed by multiregion sequencing. Nature medicine. 2015;21:751-9.

39. Shah SP, Morin RD, Khattra J, Prentice L, Pugh T, Burleigh A, Delaney A, Gelmon K, Guliany R, Senz J, Steidl C, Holt RA, Jones S, Sun M, Leung G, Moore R, Severson T, Taylor GA, Teschendorff AE, Tse K, Turashvili G, Varhol R, Warren RL, Watson P, Zhao Y, Caldas C, Huntsman D, Hirst M, Marra MA, Aparicio S. Mutational evolution in a lobular breast tumour profiled at single nucleotide resolution. Nature. 2009;461:809-13.

40. Nik-Zainal S, Van Loo P, Wedge DC, Alexandrov LB, Greenman CD, Lau KW, Raine K, Jones D, Marshall J, Ramakrishna M, Shlien A, Cooke SL, Hinton J, Menzies A, Stebbings LA, Leroy C, Jia M, Rance R, Mudie LJ, Gamble SJ, Stephens PJ, McLaren S, Tarpey PS, Papaemmanuil E, Davies HR, Varela I, McBride DJ, Bignell GR, Leung K, Butler AP, Teague JW, Martin S, Jonsson G, Mariani O, Boyault S, Miron P, Fatima A, Langerod A, Aparicio SA, Tutt A, Sieuwerts AM, Borg A, Thomas G, Salomon AV, Richardson AL, Borresen-Dale AL, Futreal PA, Stratton MR, Campbell PJ, Breast Cancer Working Group of the International Cancer Genome C. The life history of 21 breast cancers. Cell. 2012;149:994-1007.

41. Stephens PJ, Tarpey PS, Davies H, Van Loo P, Greenman C, Wedge DC, Nik-Zainal S, Martin S, Varela I, Bignell GR, Yates LR, Papaemmanuil E, Beare D, Butler A, Cheverton A, Gamble J, Hinton J, Jia M, Jayakumar A, Jones D, Latimer C, Lau KW, McLaren S, McBride DJ, Menzies A, Mudie L, Raine K, Rad R, Chapman MS, Teague J, Easton D, Langerod A, Oslo Breast Cancer C, Lee MT, Shen CY, Tee BT, Huimin BW, Broeks A, Vargas AC, Turashvili G, Martens J, Fatima A, Miron P, Chin SF, Thomas G, Boyault S, Mariani O, Lakhani SR, van de Vijver M, van 't Veer L, Foekens J, Desmedt C, Sotiriou C, Tutt A, Caldas C, Reis-Filho JS, Aparicio SA, Salomon AV, Borresen-Dale AL, Richardson AL, Campbell PJ, Futreal PA, Stratton

MR. The landscape of cancer genes and mutational processes in breast cancer. Nature. 2012;486:400-4.

42. Cheng DT, Mitchell TN, Zehir A, Shah RH, Benayed R, Syed A, Chandramohan R, Liu ZY, Won HH, Scott SN, Brannon AR, O'Reilly C, Sadowska J, Casanova J, Yannes A, Hechtman JF, Yao J, Song W, Ross DS, Oultache A, Dogan S, Borsu L, Hameed M, Nafa K, Arcila ME, Ladanyi M, Berger MF. Memorial Sloan Kettering-Integrated Mutation Profiling of Actionable Cancer Targets (MSK-IMPACT): A Hybridization Capture-Based Next-Generation Sequencing Clinical Assay for Solid Tumor Molecular Oncology. The Journal of molecular diagnostics : JMD. 2015;17:251-64.

43. De Mattos-Arruda L, Bidard FC, Won HH, Cortes J, Ng CK, Peg V, Nuciforo P, Jungbluth AA, Weigelt B, Berger MF, Seoane J, Reis-Filho JS. Establishing the origin of metastatic deposits in the setting of multiple primary malignancies: the role of massively parallel sequencing. Molecular oncology. 2014;8:150-8.

44. Toy W, Shen Y, Won H, Green B, Sakr RA, Will M, Li Z, Gala K, Fanning S, King TA, Hudis C, Chen D, Taran T, Hortobagyi G, Greene G, Berger M, Baselga J, Chandarlapaty S. ESR1 ligand-binding domain mutations in hormone-resistant breast cancer. Nature genetics. 2013;45:1439-45.

45. Li S, Shen D, Shao J, Crowder R, Liu W, Prat A, He X, Liu S, Hoog J, Lu C, Ding L, Griffith OL, Miller C, Larson D, Fulton RS, Harrison M, Mooney T, McMichael JF, Luo J, Tao Y, Goncalves R, Schlosberg C, Hiken JF, Saied L, Sanchez C, Giuntoli T, Bumb C, Cooper C, Kitchens RT, Lin A, Phommaly C, Davies SR, Zhang J, Kavuri MS, McEachern D, Dong YY, Ma C, Pluard T, Naughton M, Bose R, Suresh R, McDowell R, Michel L, Aft R, Gillanders W, DeSchryver K, Wilson RK, Wang S, Mills GB, Gonzalez-Angulo A, Edwards JR, Maher C, Perou CM, Mardis ER, Ellis MJ. Endocrine-therapy-resistant ESR1 variants revealed by genomic characterization of breast-cancer-derived xenografts. Cell reports. 2013;4:1116-30.

46. Schiavon G, Hrebien, S., Garcia-Murillas, I., Pearson, A., Tarazona, N., Lopez-Knowles, E., Ribas, R., Nerurkar, A., Osin, P., Martin, L-A., Dowsett, M., Smith, I.E., Turner, N.C. . ESR1 mutations evolve during the treatment of metastatic breast cancer, and detection in ctDNA predicts sensitivity to subsequent hormone therapy. [abstract]. In: Proceedings of the 106th Annual Meeting of the American Association for Cancer Research. Cancer Res 2015;75(15 Suppl):Abstract nr 926. 2015.

47. Tanaka S, Louis DN, Curry WT, Batchelor TT, Dietrich J. Diagnostic and therapeutic avenues for glioblastoma: no longer a dead end? Nature reviews Clinical oncology. 2013;10:14-26.

48. Brastianos PK, Carter SL, Santagata S, Cahill DP, Taylor-Weiner A, Jones RT, Van Allen EM, Lawrence MS, Horowitz PM, Cibulskis K, Ligon KL, Tabernero J, Seoane J, Martinez-Saez E, Curry WT, Dunn IF, Paek SH, Park SH, McKenna A, Chevalier A, Rosenberg M, Barker FG, 2nd, Gill CM, Van Hummelen P, Thorner AR, Johnson BE, Hoang MP, Choueiri TK, Signoretti S, Sougnez C, Rabin MS, Lin NU, Winer EP, Stemmer-Rachamimov A, Meyerson M, Garraway L, Gabriel S, Lander ES, Beroukhim R, Batchelor TT, Baselga J, Louis DN, Getz G, Hahn WC. Genomic Characterization of Brain Metastases Reveals Branched Evolution and Potential Therapeutic Targets. Cancer discovery. 2015;5:1164-77.

49. Neagu MR, Gill CM, Batchelor TT, Brastianos PK. Genomic profiling of brain metastases: current knowledge and new frontiers. Chinese clinical oncology. 2015;4:22.

50. Owonikoko TK, Arbiser J, Zelnak A, Shu HK, Shim H, Robin AM, Kalkanis SN, Whitsett TG, Salhia B, Tran NL, Ryken T, Moore MK, Egan KM, Olson JJ. Current approaches to the treatment of metastatic brain tumours. Nature reviews Clinical oncology. 2014;11:203-22.

51. Shi R, Wang PY, Li XY, Chen JX, Li Y, Zhang XZ, Zhang CG, Jiang T, Li WB, Ding W, Cheng SJ. Exosomal levels of miRNA-21 from cerebrospinal fluids associated with poor prognosis and tumor recurrence of glioma patients. Oncotarget. 2015;6:26971-81.

52. Johnson BE, Mazor T, Hong C, Barnes M, Aihara K, McLean CY, Fouse SD, Yamamoto S, Ueda H, Tatsuno K, Asthana S, Jalbert LE, Nelson SJ, Bollen AW, Gustafson WC, Charron E, Weiss WA, Smirnov IV, Song JS, Olshen AB, Cha S, Zhao Y, Moore RA, Mungall AJ, Jones SJ, Hirst M, Marra MA, Saito N, Aburatani H, Mukasa A, Berger MS, Chang SM, Taylor BS, Costello JF. Mutational analysis reveals the origin and therapy-driven evolution of recurrent glioma. Science. 2014;343:189-93.

53. Ding L, Ellis MJ, Li S, Larson DE, Chen K, Wallis JW, Harris CC, McLellan MD, Fulton RS, Fulton LL, Abbott RM, Hoog J, Dooling DJ, Koboldt DC, Schmidt H, Kalicki J, Zhang Q, Chen L, Lin L, Wendl MC, McMichael JF, Magrini VJ, Cook L, McGrath SD, Vickery TL, Appelbaum E, Deschryver K, Davies S, Guintoli T, Lin L, Crowder R, Tao Y, Snider JE, Smith SM, Dukes AF, Sanderson GE, Pohl CS, Delehaunty KD, Fronick CC, Pape KA, Reed JS, Robinson JS, Hodges JS, Schierding W, Dees ND, Shen D, Locke DP, Wiechert ME, Eldred JM, Peck JB, Oberkfell BJ, Lolofie JT, Du F, Hawkins AE, O'Laughlin MD, Bernard KE, Cunningham M, Elliott G, Mason MD, Thompson DM, Jr., Ivanovich JL, Goodfellow PJ, Perou CM, Weinstock GM, Aft R, Watson M, Ley TJ, Wilson RK, Mardis ER. Genome remodelling in a basal-like breast cancer metastasis and xenograft. Nature. 2010;464:999-1005.

54. Saunus JM, Quinn MC, Patch AM, Pearson JV, Bailey PJ, Nones K, McCart Reed AE, Miller D, Wilson PJ, Al-Ejeh F, Mariasegaram M, Lau Q, Withers T, Jeffree RL, Reid LE, Silva

LD, Matsika A, Niland CM, Cummings MC, Bruxner TJ, Christ AN, Harliwong I, Idrisoglu S, Manning S, Nourse C, Nourbakhsh E, Wani S, Anderson MJ, Lynn Fink J, Holmes O, Kazakoff S, Leonard C, Newell F, Taylor D, Waddell N, Wood S, Xu Q, Kassahn KS, Narayanan V, Taib NA, Teo SH, Chow YP, kConFab, Jat PS, Brandner S, Flanagan AM, Khanna K, Chenevix-Trench G, Grimmond SM, Simpson PT, Waddell N, Lakhani SR. Integrated genomic and transcriptomic analysis of human brain metastases identifies alterations of potential clinical significance. The Journal of pathology. 2015.

55. Paik PK, Shen R, Won H, Rekhtman N, Wang L, Sima CS, Arora A, Seshan V, Ladanyi M, Berger MF, Kris MG. Next-Generation Sequencing of Stage IV Squamous Cell Lung Cancers Reveals an Association of PI3K Aberrations and Evidence of Clonal Heterogeneity in Patients with Brain Metastases. Cancer discovery. 2015;5:610-21.

Appendices I

Appendices Figure A1

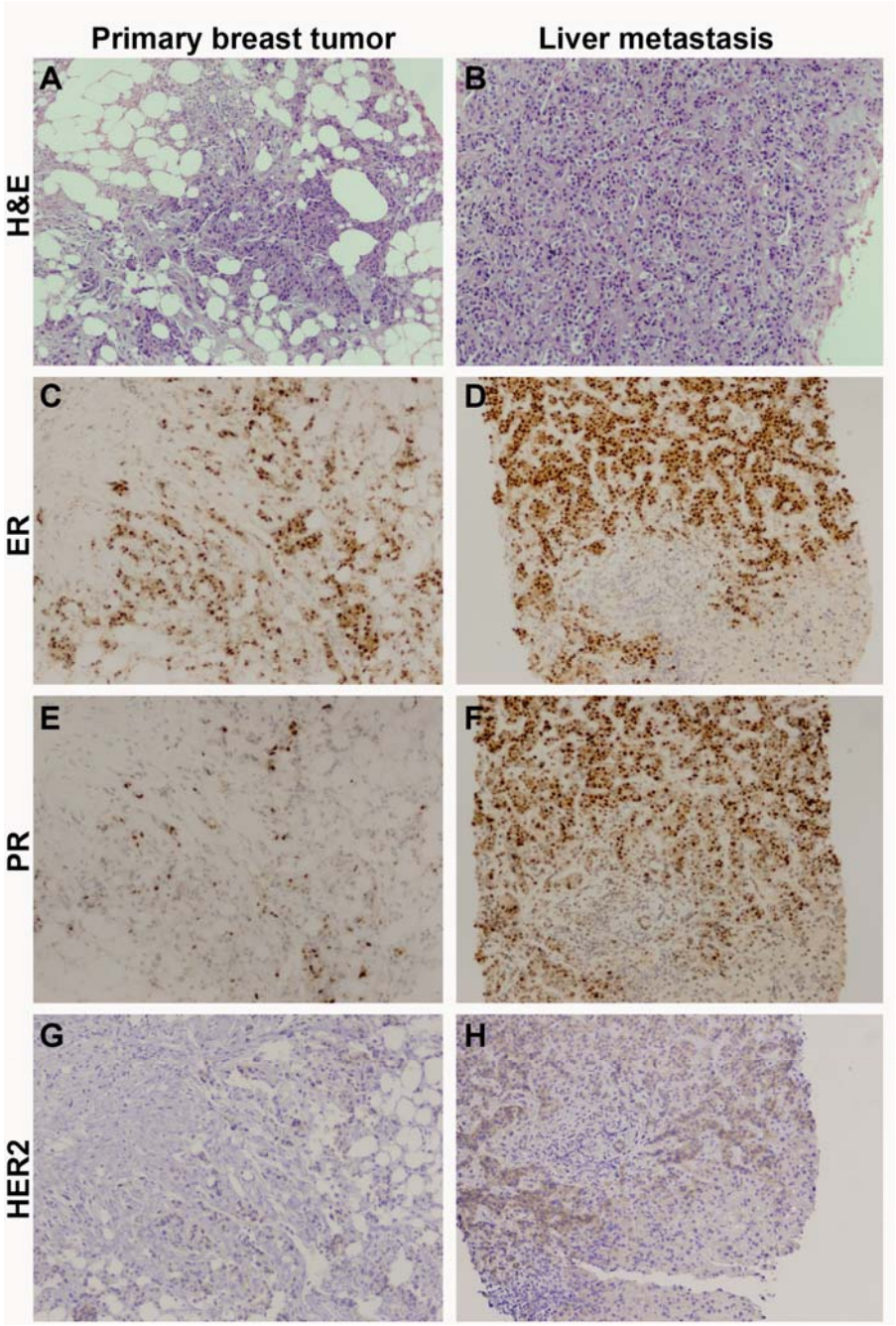

Appendices Figure A1. Representative micrographs of the primary breast cancer (A, C, E, G) and its liver metastasis (B, D, F, H). Both the primary breast cancer and its liver metastasis are estrogen receptor (ER)-positive, progesterone receptor (PR) positive and HER2-negative. A and B, Hematoxylin & eosin staining; C and D, ER immunohistochemistry (Novocastra, Leica Biosystems Newcastle Ltd, UK, 6F11, 7 ml Bond ready-to-use, Heat Induced Epitope Retrieval (HIER) pH 9); E and F, PR immunohistochemistry (Novocastra, Leica Biosystems Newcastle Ltd, UK, SAN27, 7 ml Bond ready-touse, HIER pH 6); G and H, HER2 immunohistochemistry (PATHWAY® HER2, clone 4B5; Ventana Medical Systems Inc., Tucson, AZ). Original magnification10x.

Appendices Table A1. Patients' clinical details.

Case	Tumour type	Biopsy site	Clinical summary
GBM1	Glioblastoma	Brain tumour (secondary GBM)	33 year-old woman with diffuse low-grade astrocytoma in the right frontal and temporal lobes. The patient was operated and received chemotherapy and WBRT. After 5 years free of disease, she developed neurologic symptoms and had documented recurrence on MRI. Following treatment with temozolomide, she progressed later on and she was subjected to partial resection of the brain tumour, which showed evidence of secondary glioblastoma, IDH1 positive. Patient had fast clinical deterioration and received palliative care until she passed away.
GBM2	Glioblastoma	Primary brain tumour	52 year-old man with diagnosis of glioblastoma. Following partial resection of the brain tumour, patient received WBRT plus concomitant and adjuvant temozolomide. He progressed months later as observed on MRI. After clinical deterioration, he received palliative care until he passed away.
GBM3	Glioblastoma	Primary brain tumour	64 year-old woman with diagnosis of temporal glioblastoma (IDH1 negative, *EGFR* mutant). She was subjected to partial resection of the brain tumour. Then, she was treated with a targeted therapy plus temozolomide, concomitantly with WBRT.

GBM4	Glioblastoma	Primary brain tumour (secondary GBM)	54 year-old man with anaplastic astrocytoma. The tumour was subjected to suboptimal exeresis and the patient received chemotherapy and WBRT. After 12 months, a new exeresis was performed which showed evidence of secondary glioblastoma. Patient received a new line of chemotherapy, and upon progression, was enrolled in a clinical trial. Patient had no clinical benefit and passed away.
BMBC1	Metastatic breast cancer	Brain metastasis	56 year-old woman diagnosed with ductal invasive ER-positive, HER2-negative early breast cancer (T2N0M0). After 10 years, she developed bone metastasis. She received multiple lines of treatments with stable disease for 33 months when she presented neurologic symptoms. Following MRI and serial cytological spinal fluid examination, a diagnosis of leptomeningeal carcinomatosis was established and WBRT was administered. Further disease progression in the brain was observed and the patient was enrolled in a palliative care program due to poor performance status.
BMBC2	Metastatic breast cancer	Meningeal implants	35 year-old woman diagnosed with ductal invasive ER-positive, HER2-negative breast cancer (T1cN0M0) in 2007. She had breast conservative surgery and received standard adjuvant therapy. In 2010, a biopsy confirmed bone metastasis and the patient received endocrine-based therapy and local RT. After multiple lines of endocrine, chemotherapy and targeted therapy due to bone and lung progression, the patient developed neurologic symptoms. Signs of leptomeningeal carcinomatosis were detected on the MRI but three serial spinal fluid cytological analyses were negative. After WBRT and a new line of chemotherapy, visceral disease progression was observed.
BMBC3	Metastatic breast cancer	Brain metastasis and meningeal implants	33 year-old woman diagnosed with ductal invasive carcinoma ER-positive, HER2-positive breast cancer (cT2N2M1) in 2006. The patient received first-line therapy with the anti-HER2 trastuzumab and chemotherapy, achieving almost complete response. After bone progression, she received multiple lines of trastuzumab combined with endocrine or chemotherapy. Subsequently, a diagnosis of Li-Fraumeni syndrome (germline *TP53* mutation) was confirmed. In 2009, she presents disease progression in CNS, bone and breast received WBRT and was treated with targeted therapies. In 2012, due to a right nasal cavity mass and palpable cervical lymph node, a diagnosis of a secondary primary tumour (esthesioneuroblastoma) was made and the patient received local RT combined with cisplatin and

			etoposide. Further disease progression was observed in brain, bone (a biopsy was done and had HER2-positive status) and visceral sites and the patient received further lines with cytotoxic agent and anti-HER2 therapy.
BMBC4	Metastatic breast cancer	Meningeal implants	43 year-old woman diagnosed with locally advanced ductal invasive ER-positive, HER2-positive breast cancer (cT4bN2M0) in 2006. After neoadjuvant chemotherapy, patient was submitted to mastectomy, adjuvant endocrine treatment, and trastuzumab. In 2009, she developed bone and liver metastases and received several lines of anti-HER2-based systemic therapies, including a targeted therapy and trastuzumab. After presenting mentonian paresthesias, leptomeningeal carcinomatosis was clinically diagnosed and treated with WBRT. Two months after the patient passed away.
BMBC5	Metastatic breast cancer	Brain metastasis	36 year-old woman diagnosed with invasive ductal carcinoma ER-negative, HER2-positive breast cancer (cT3N3M1) in 2012. The patient received first-line therapy with the anti-HER2 trastuzumab plus paclitaxel; following successive visceral and brain progression (2013), patient received WBRT and more 3 lines of anti-HER2 therapies combined with cytotoxic and targeted agents until she passed away in 2014.
BMBC6	Metastatic breast cancer	Brain metastasis	37 year-old woman diagnosed with invasive ductal carcinoma ER-positive (pT2N1M0) in 1993. She had a mastectomy and received standard adjuvant therapy. In 1995, bone metastasis was diagnosed and the patient received endocrine-based therapy and local RT. In 2013, after multiple lines of endocrine, chemotherapy and targeted therapy due to bone and hepatic progression, the patient developed neurologic symptoms. A brain MRI confirmed the diagnosis of brain metastases and WBRT was administered. Patient received a new line of chemotherapy and passed away.
BMLC1	Non-small cell lung cancer	Brain metastasis	36 year-old woman with non-small cell lung adenocarcinoma (stage IV, *EGFR* mutation). Patient was subjected to partial resection of thoracic disease (lobectomy and pleural implants) and received post-operative chemotherapy. Following new surgical intervention, received another post-operative chemotherapy. After disease progression, she received treatment with erlotinib. After two years, she developed neurologic symptoms and had documented progressive disease documented in brain MRI. She was subjected to incomplete resection

			of the left parietal-occipital brain metastasis, which harbored an activating *EGFR* mutation (exon 21) and carried on treatment with erlotinib. Following brain RT, and due to persistence of brain disease on MRI, patient was operated again. After two months, patient had evidence of progressive disease in mediastinum and was treated with targeted therapies. Patient had partial response in mediastinum and no evidence of recurrence in the brain.
BMLC2	Non-small cell lung cancer	Brain metastasis	69 year-old man with non-small cell lung adenocarcinoma. Patient was operated (pT2N2M0, *EGFR* and *ALK* negative) and kept in clinic-radiological follow up. Four months after, he developed neurologic symptoms and had documented progressive disease on brain MRI. He was subjected to complete resection of the left temporal brain metastasis, and further received WBRT, being disease free.
BMLC3	Non-small cell lung cancer	Brain metastasis	65 year-old man with non-small cell lung adenocarcinoma (T4N3M0). The patient is treated with chemotherapy and radiotherapy, achieving complete response. Twelve months after, he developed neurologic symptoms and had documented progressive disease on brain MRI. He was subjected to complete resection of the cerebellar brain metastasis, being disease free.

Abbreviations: ALK, anaplastic lymphoma kinase; CNS, central nervous system; EGFR, epidermal growth factor receptor; ER, estrogen receptor, GBM, glioblastoma; MRI, magnetic resonance imaging; WBRT, whole brain radiotherapy.

Appendices Table A2. Tumour burden of patients with central nervous system disease (CNS)-restricted disease and CNS and non-CNS (disseminated disease).

Case	**Site of metastases**	**Lesions on last imaging scans**
CNS restricted		
GBM1	CNS	Lesion in the right frontal lobe (55x60mm)

GBM2	CNS	Lesion in the corpus callosum (39x16x19 mm).
GBM3	CNS	Lesion in the left temporal lobe (50x28 mm).
GBM4	CNS	Right parieto-occipital mass (85x58x53 mm).
BMBC1	CNS	Right thalamic mass (5.6 x 4.2mm), meningeal implants (not measurable).
	Non-CNS	Mild pleural, pericardial implants and bone metastasis (not measurable).
BMBC5	CNS	Multiple supra and infratentorial brain metastases: left frontal (15x19 mm), right parietal (13x24mm), basal ganglia (12x10 mm), occipital (10x8 mm).
	Non-CNS	Hepatic subcentimeter lesion in segment IV.
BMLC3	CNS	Pre-surgical cerebellar brain metastasis (37x33x34 mm).
	Non-CNS	No evidence of thoracic disease.
CNS and non-CNS (disseminated disease)		
BMBC2	CNS	Meningeal implants in left and right parietal convexity.
	Non-CNS	Liver with about 60-70% of the parenchyma involved with metastasis (greater lesions: 43x40mm and 27x27mm, liver longer axis 27cm), pleural and abdominal effusion and multiple bone metastases (not measurable).

BMBC3	CNS	Left temporo-occipital (30x16mm), right frontal (7x6 mm), extra-parenchymatous falx cerebri (10x11mm), esphenoidal lesion (not measurable).
	Non- CNS	Moderate left pleural effusion, hepatic subcentimeter lesion in segment II, multiple bone metastases (not measurable).
BMBC4	CNS	Meningeal implants in brain and cervical spinal cord (not measurable).
	Non-CNS	Liver (21x18mm, 15x21mm, 39x15mm, 29x22mm, and others - longer axis 21cm, 30-40% parenchyma involved), para-tracheal lymph node (8x7mm), peri-pancreatic lymph node (13x10mm), multiple bone metastases (not measurable).
BMBC6	CNS	Pre and post central gyrus lesions (18x18 mm), multiple left fronto-parietal gyrus lesions, posterior fossa (vermis lesion 3 mm).
	Non-CNS	Multiple liver metastases: segment V/VIII (69x55 mm), segment IV (59x43 mm), segment III (18x17mm). Peritoneal implants and multiple bone metastases (not measurable).
BMLC1	CNS	Left parieto-temporal brain lesion (32x23x26 mm) and left parieto-occipital lesion (27x14 mm).
	Non-CNS	Pulmonary lesion in left upper lobe (5.8x4 mm).

Appendices Table A3. Expansion cohort of patients in which CSF ctDNA and plasma ctDNA are compared.

Patient ID	**Tumour Type**
Brain metastasis from breast cancer	
BMBC7	Brain metastasis from ER-positive / HER2-negative breast cancer
BMBC8	Brain metastasis from ER-negative / HER2-negative breast cancer
BMBC9	Brain metastasis from ER-positive / HER2-negative breast cancer
BMBC10	Brain metastasis from ER-positive / HER2-negative breast cancer
Brain metastasis from lung cancer	

BMLC4	Non-small cell lung cancer (large cell carcinoma)
BMLC5	Non-small cell lung cancer (adenocarcinoma, *KRAS* mutation)
BMLC6	Non-small cell lung cancer (large cell carcinoma)
BMLC7	Non-small cell lung adenocarcinoma (*ALK* translocation)
BMLC8	Non-small cell lung adenocarcinoma
Primary brain tumours	
Medullo1	Medulloblastoma (classic type)
Medullo2	Medulloblastoma (anaplastic type)

Appendices Table A4. Analysis of sensitivity for central nervous system (CNS) and non-CNS disease, CSF ctDNA and plasma ctDNA.

CNS restricted					
	MSK-IMPACT	**MSK-IMPACT and breast panel**	**N of all SNVs and indels**	**Present in CSF and CNS**	**Present in plasma and CNS**
GBM1	Yes		5	1/3 (33.3%)	0/3 (0%)
GBM2	Yes		3	1/3 (33.3%)	0/3 (0%)
GBM3	Yes		1	1/1 (100%)	0/1 (0%)
GBM4	Yes		4	1/2 (50%)	0/2 (0%)
BMBC1		Yes	21	6/7 (85.7%)	0/7 (0%)
BMBC5	Yes		15	4/15 (26.6%)	0/15 (0%)
BMLC3	Yes		9	7/9 (77.8%)	0/9 (0%)
Mean			8.4	58%	0%
CNS and non-CNS (disseminated disease)					
BMBC2		Yes	28	6/16 (37.5%)	6/16 (37.5%)
BMBC3		Yes	17	6/16 (100%)	3/16 (50%)
BMBC4		Yes	16	3/5 (60%)	5/5 (100%)
BMBC6	Yes		18	8/10 (80%)	9/10 (90%)
BMLC1	Yes		4	1/4 (25%)	0/4 (0%)
Mean			16.6	60.5%	55.5%

Appendices Table A5. Tumour volume measurements as per computer aided planimetric analyses.

Patient ID	Volume of brain lesions (cm^3)	
	Time Point 1	Time Point 2
GBM1	82.24	70.32
GBM2	N/A	8.98
GBM3	49.36	4.7
BMLC1	20.99	0
BMLC2	6.71	0

Abbreviation: N/A, not available.

Appendices Table A6. Gene mutations and their respective mutant allelic frequencies in the CSF ctDNA and plasma ctDNA as determined per digital PCR.

Case	Gene	Amino acid Change	CSF 1	CSF 2	Plasma 1	Plasma 2
GBM1	IDH1	R132H	21.8%	22.7%	0.0%	N/A
	TP53	R114C	40.0%	42.0%	0.0%	N/A
	ANK2	K2337X	30.0%	27.2%	0.0%	N/A
GBM2	EGFR	C620S	2.9%	N/A	0.4%	N/A
	PTEN	D162V	0.8%	N/A	0.0%	N/A
GBM3	EGFR	R108K	92.6%	0.0%	0.3%	0.0%
	FTH1	I146T	2.0%	0.0%	0.0%	0.0%
	OR51D1	R135C	17.0%	0.0%	0.0%	0.0%
BMBC1	POLE	E318K	22.8%	70.9%	10.7%	1.0%
	ARID5B	E572K	22.2%	30.9%	9.8%	2.0%
	PCDH1	S190C	38.8%	77.9%	13.6%	2.0%
BMLC1	CD9	W22L	0.2%	0.0%	0.0%	0.2%
	EGFR	L858R	0.1%	0.0%	0.0%	0.0%
BMLC2	ADAMTS12	T982K	15.5%	0.0%	0.0%	0.2%
	AHRR	G353C	20.8%	0.0%	0.0%	0.0%
Median (range)	-	-	20.8% (0.1-92.6)	0% (0-77.9)	0% (0-13.6)	0.1% (0-2.0)

Abbreviation: N/A, not available.

Appendices Supplementary Data 1. List of the customized breast cancer and MSK-IMPACT platforms (254 breast cancer-associated genes and 341 cancer-associated genes) involved in the targeted capture massively parallel sequencing employed in these studies.

MSK-IMPACT panel	Breast Panel	Unique genes to both panels	Common genes to both panels
ABL1	ABCA13	ABL1	AKT1
AKT1	ABCB1	AKT1	AKT2
AKT2	ADAMTSL1	AKT2	AKT3
AKT3	AGFG2	AKT3	APC
ALK	AHNAK2	ALK	ARAF
ALOX12B	AK9	ALOX12B	ARID1A
APC	AKAP9	APC	ATM
AR	AKT1	AR	ATR
ARAF	AKT2	ARAF	ATRX
ARID1A	AKT3	ARID1A	AURKA
ARID1B	ANK3	ARID1B	AURKB
ARID2	AOAH	ARID2	BRAF
ARID5B	APC	ARID5B	BRCA1
ASXL1	APOBEC1	ASXL1	BRCA2
ASXL2	APOBEC2	ASXL2	BRIP1
ATM	APOBEC3A	ATM	CBFB
ATR	APOBEC3C	ATR	CDH1
ATRX	APOBEC3D	ATRX	CDK4
AURKA	APOBEC3F	AURKA	CDK6
AURKB	APOBEC3G	AURKB	CDKN1A
AXIN1	APOBEC3H	AXIN1	CDKN1B
AXIN2	APOBEC4	AXIN2	CDKN2A
AXL	ARAF	AXL	CDKN2B
B2M	ARID1A	B2M	CHEK1
BAP1	ATM	BAP1	CHEK2
BARD1	ATN1	BARD1	CTCF
BBC3	ATR	BBC3	CTNNB1
BCL2	ATRX	BCL2	EGFR
BCL2L1	AURKA	BCL2L1	ERBB2
BCL2L11	AURKB	BCL2L11	ERBB3
BCL6	AURKC	BCL6	ERBB4
BCOR	BIRC5	BCOR	ERCC2
BLM	BRAF	BLM	ERCC3
BMPR1A	BRCA1	BMPR1A	ERCC5

BRAF	BRCA2	BRAF	ESR1
BRCA1	BRIP1	BRCA1	FANCA
BRCA2	CACNA1A	BRCA2	FANCC
BRD4	CACNA1C	BRD4	FGFR1
BRIP1	CACNA1E	BRIP1	FGFR2
BTK	CBFB	BTK	FGFR3
CARD11	CDC25A	CARD11	FGFR4
CASP8	CDC25B	CASP8	FOXA1
CBFB	CDC25C	CBFB	GATA3
CBL	CDH1	CBL	GRIN2A
CCND1	CDK1	CCND1	HIST1H3B
CCND2	CDK4	CCND2	HRAS
CCND3	CDK6	CCND3	IGF1R
CCNE1	CDKN1A	CCNE1	INPP4B
CD274	CDKN1B	CD274	IRS1
CD276	CDKN2A	CD276	JAK1
CD79B	CDKN2B	CD79B	JAK2
CDC73	CEP164	CDC73	KIT
CDH1	CHD4	CDH1	KMT2C
CDK12	CHD6	CDK12	KMT2D
CDK4	CHEK1	CDK4	KRAS
CDK6	CHEK2	CDK6	MAP2K1
CDK8	COL12A1	CDK8	MAP2K2
CDKN1A	CTCF	CDKN1A	MAP2K4
CDKN1B	CTNNB1	CDKN1B	MAP3K1
CDKN2A	CUBN	CDKN2A	MAPK1
CDKN2B	DCHS2	CDKN2B	MDM2
CDKN2C	DCLRE1C	CDKN2C	MED12
CHEK1	DEPTOR	CHEK1	MET
CHEK2	DMC1	CHEK2	MLH1
CIC	DOCK11	CIC	MRE11A
CREBBP	EGFR	CREBBP	MSH2
CRKL	EIF4A2	CRKL	MSH6
CRLF2	EME1	CRLF2	MTOR
CSF1R	EME2	CSF1R	MUTYH
CTCF	EPPK1	CTCF	NBN
CTLA4	ERBB2	CTLA4	NCOR1
CTNNB1	ERBB3	CTNNB1	NF1
CUL3	ERBB4	CUL3	NF2
DAXX	ERCC1	DAXX	NRAS
DCUN1D1	ERCC2	DCUN1D1	PALB2

DDR2	ERCC3	DDR2	PARP1
DICER1	ERCC5	DICER1	PDGFRA
DIS3	ESR1	DIS3	PDGFRB
DNMT1	ESR2	DNMT1	PIK3CA
DNMT3A	FAM157B	DNMT3A	PIK3CB
DNMT3B	FANCA	DNMT3B	PIK3R1
DOT1L	FANCB	DOT1L	PMS1
E2F3	FANCC	E2F3	PMS2
EED	FANCD2	EED	POLE
EGFL7	FANCE	EGFL7	PTCH1
EGFR	FANCF	EGFR	PTEN
EIF1AX	FANCG	EIF1AX	RAD50
EP300	FANCI	EP300	RAD51
EPCAM	FANCL	EPCAM	RAD51B
EPHA3	FANCM	EPHA3	RAD51C
EPHA5	FBN1	EPHA5	RAD51D
EPHB1	FGFR1	EPHB1	RAD52
ERBB2	FGFR2	ERBB2	RAD54L
ERBB3	FGFR3	ERBB3	RAF1
ERBB4	FGFR4	ERBB4	RB1
ERCC2	FMN2	ERCC2	RICTOR
ERCC3	FOXA1	ERCC3	RPTOR
ERCC4	FOXC2	ERCC4	RUNX1
ERCC5	FRG1B	ERCC5	SF3B1
ERG	GATA3	ERG	SMO
ESR1	GPS2	ESR1	SPEN
ETV1	GRB2	ETV1	TBX3
ETV6	GRIN2A	ETV6	TGFBR1
EZH2	GRIN2B	EZH2	TGFBR2
FAM123B	HECW1	FAM123B	TP53
FAM175A	HERC2	FAM175A	TSC1
FAM46C	HIF1A	FAM46C	TSC2
FANCA	HIST1H3B	FANCA	
FANCC	HRAS	FANCC	
FAT1	HRNR	FAT1	
FBXW7	HSP90AA1	FBXW7	
FGF19	HSP90AB1	FGF19	
FGF3	HUWE1	FGF3	
FGF4	IGF1R	FGF4	
FGFR1	INPP4B	FGFR1	
FGFR2	IRS1	FGFR2	

FGFR3	JAK1	FGFR3	
FGFR4	JAK2	FGFR4	
FH	KIT	FH	
FLCN	KMT2C	FLCN	
FLT1	KMT2D	FLT1	
FLT3	KRAS	FLT3	
FLT4	LAMA1	FLT4	
FOXA1	LAMA5	FOXA1	
FOXL2	MACF1	FOXL2	
FOXP1	MAP1A	FOXP1	
FUBP1	MAP2K1	FUBP1	
GATA1	MAP2K2	GATA1	
GATA2	MAP2K3	GATA2	
GATA3	MAP2K4	GATA3	
GNA11	MAP2K6	GNA11	
GNAQ	MAP3K1	GNAQ	
GNAS	MAP3K10	GNAS	
GREM1	MAP3K4	GREM1	
GRIN2A	MAP4K4	GRIN2A	
GSK3B	MAPK1	GSK3B	
H3F3C	MAPK8	H3F3C	
HGF	MAPK9	HGF	
HIST1H1C	MDM2	HIST1H1C	
HIST1H2BD	MDN1	HIST1H2BD	
HIST1H3B	MED12	HIST1H3B	
HNF1A	MET	HNF1A	
HRAS	MGAM	HRAS	
ICOSLG	MGMT	ICOSLG	
IDH1	MLH1	IDH1	
IDH2	MLH3	IDH2	
IFNGR1	MRE11A	IFNGR1	
IGF1	MSH2	IGF1	
IGF1R	MSH3	IGF1R	
IGF2	MSH5	IGF2	
IKBKE	MSH6	IKBKE	
IKZF1	MST1L	IKZF1	
IL10	MTOR	IL10	
IL7R	MUTYH	IL7R	
INPP4A	MXRA5	INPP4A	
INPP4B	MYB	INPP4B	
INSR	NBEAL2	INSR	

IRF4	NBN	IRF4	
IRS1	NBPF1	IRS1	
IRS2	NCOA3	IRS2	
JAK1	NCOR1	JAK1	
JAK2	NCOR2	JAK2	
JAK3	NEB	JAK3	
JUN	NF1	JUN	
KDM5A	NF2	KDM5A	
KDM5C	NR1H2	KDM5C	
KDM6A	NRAS	KDM6A	
KDR	PALB2	KDR	
KEAP1	PARP1	KEAP1	
KIT	PARP2	KIT	
KLF4	PARP3	KLF4	
KRAS	PAXIP1	KRAS	
LATS1	PCNXL2	LATS1	
LATS2	PDGFRA	LATS2	
LMO1	PDGFRB	LMO1	
MAP2K1	PGR	MAP2K1	
MAP2K2	PIK3CA	MAP2K2	
MAP2K4	PIK3CB	MAP2K4	
MAP3K1	PIK3R1	MAP3K1	
MAP3K13	PLEC	MAP3K13	
MAPK1	PLK1	MAPK1	
MAX	PLXNA4	MAX	
MCL1	PMS1	MCL1	
MDC1	PMS2	MDC1	
MDM2	POLB	MDM2	
MDM4	POLD1	MDM4	
MED12	POLE	MED12	
MEF2B	POLH	MEF2B	
MEN1	POLQ	MEN1	
MET	PRKCA	MET	
MITF	PRKCB	MITF	
MLH1	PRKCD	MLH1	
MLL	PRKCG	MLL	
KMT2C	PRKD1	KMT2C	
KMT2D	PTCH1	KMT2D	
MPL	PTEN	MPL	
MRE11A	PTK2	MRE11A	
MSH2	RAD50	MSH2	

MSH6	RAD51	MSH6	
MTOR	RAD51B	MTOR	
MUTYH	RAD51C	MUTYH	
MYC	RAD51D	MYC	
MYCL1	RAD52	MYCL1	
MYCN	RAD54B	MYCN	
MYD88	RAD54L	MYD88	
MYOD1	RAF1	MYOD1	
NBN	RB1	NBN	
NCOR1	RBBP8	NCOR1	
NF1	RELN	NF1	
NF2	RICTOR	NF2	
NFE2L2	RIF1	NFE2L2	
NKX2-1	RPGR	NKX2-1	
NKX3-1	RPS6KB1	NKX3-1	
NOTCH1	RPTOR	NOTCH1	
NOTCH2	RUNX1	NOTCH2	
NOTCH3	SAAL1	NOTCH3	
NOTCH4	SF3B1	NOTCH4	
NPM1	SHC1	NPM1	
NRAS	SHROOM4	NRAS	
NSD1	SMO	NSD1	
NTRK1	SOS1	NTRK1	
NTRK2	SPEN	NTRK2	
NTRK3	SPRY1	NTRK3	
PAK1	SPTA1	PAK1	
PAK7	SRCAP	PAK7	
PALB2	STAT1	PALB2	
PARK2	STAT3	PARK2	
PARP1	SVEP1	PARP1	
PAX5	TBL1XR1	PAX5	
PBRM1	TBX3	PBRM1	
PDCD1	TENM1	PDCD1	
PDGFRA	TGFBR1	PDGFRA	
PDGFRB	TGFBR2	PDGFRB	
PDPK1	TGFBR3	PDPK1	
PHOX2B	TOP2A	PHOX2B	
PIK3C2G	TP53	PIK3C2G	
PIK3C3	TP53BP1	PIK3C3	
PIK3CA	TSC1	PIK3CA	
PIK3CB	TSC2	PIK3CB	

PIK3CD	TYK2	PIK3CD	
PIK3CG	UBR4	PIK3CG	
PIK3R1	USP36	PIK3R1	
PIK3R2	WDFY3	PIK3R2	
PIK3R3	XBP1	PIK3R3	
PIM1	XPA	PIM1	
PLK2	XPC	PLK2	
PMAIP1	XRCC1	PMAIP1	
PMS1	XRCC2	PMS1	
PMS2	XRCC3	PMS2	
PNRC1	ZFHX3	PNRC1	
POLE	ZFHX4	POLE	
PPP2R1A	ZFP36L1	PPP2R1A	
PRDM1	ZNF384	PRDM1	
PRKAR1A	ZNF703	PRKAR1A	
PTCH1		PTCH1	
PTEN		PTEN	
PTPN11		PTPN11	
PTPRD		PTPRD	
PTPRS		PTPRS	
PTPRT		PTPRT	
RAC1		RAC1	
RAD50		RAD50	
RAD51		RAD51	
RAD51B		RAD51B	
RAD51C		RAD51C	
RAD51D		RAD51D	
RAD52		RAD52	
RAD54L		RAD54L	
RAF1		RAF1	
RARA		RARA	
RASA1		RASA1	
RB1		RB1	
RBM10		RBM10	
RECQL4		RECQL4	
REL		REL	
RET		RET	
RFWD2		RFWD2	
RHOA		RHOA	
RICTOR		RICTOR	
RIT1		RIT1	

RNF43		RNF43	
ROS1		ROS1	
RPS6KA4		RPS6KA4	
RPS6KB2		RPS6KB2	
RPTOR		RPTOR	
RUNX1		RUNX1	
RYBP		RYBP	
SDHA		SDHA	
SDHAF2		SDHAF2	
SDHB		SDHB	
SDHC		SDHC	
SDHD		SDHD	
SETD2		SETD2	
SF3B1		SF3B1	
SH2D1A		SH2D1A	
SHQ1		SHQ1	
SMAD2		SMAD2	
SMAD3		SMAD3	
SMAD4		SMAD4	
SMARCA4		SMARCA4	
SMARCB1		SMARCB1	
SMARCD1		SMARCD1	
SMO		SMO	
SOCS1		SOCS1	
SOX17		SOX17	
SOX2		SOX2	
SOX9		SOX9	
SPEN		SPEN	
SPOP		SPOP	
SRC		SRC	
STAG2		STAG2	
STK11		STK11	
STK40		STK40	
SUFU		SUFU	
SUZ12		SUZ12	
SYK		SYK	
TBX3		TBX3	
TERT		TERT	
TET1		TET1	
TET2		TET2	
TGFBR1		TGFBR1	

TGFBR2		TGFBR2	
TMEM127		TMEM127	
TMPRSS2		TMPRSS2	
TNFAIP3		TNFAIP3	
TNFRSF14		TNFRSF14	
TOP1		TOP1	
TP53		TP53	
TP63		TP63	
TRAF7		TRAF7	
TSC1		TSC1	
TSC2		TSC2	
TSHR		TSHR	
U2AF1		U2AF1	
VHL		VHL	
VTCN1		VTCN1	
WT1		WT1	
XIAP		XIAP	
XPO1		XPO1	
YAP1		YAP1	
YES1		YES1	
		ABCA13	
		ABCB1	
		ADAMTSL1	
		AGFG2	
		AHNAK2	
		AK9	
		AKAP9	
		ANK3	
		AOAH	
		APOBEC1	
		APOBEC2	
		APOBEC3A	
		APOBEC3C	
		APOBEC3D	
		APOBEC3F	
		APOBEC3G	
		APOBEC3H	
		APOBEC4	
		ATN1	
		AURKC	
		BIRC5	

		CACNA1A	
		CACNA1C	
		CACNA1E	
		CDC25A	
		CDC25B	
		CDC25C	
		CDK1	
		CEP164	
		CHD4	
		CHD6	
		COL12A1	
		CUBN	
		DCHS2	
		DCLRE1C	
		DEPTOR	
		DMC1	
		DOCK11	
		EIF4A2	
		EME1	
		EME2	
		EPPK1	
		ERCC1	
		ESR2	
		FAM157B	
		FANCB	
		FANCD2	
		FANCE	
		FANCF	
		FANCG	
		FANCI	
		FANCL	
		FANCM	
		FBN1	
		FMN2	
		FOXC2	
		FRG1B	
		GPS2	
		GRB2	
		GRIN2B	
		HECW1	
		HERC2	

		HIF1A	
		HRNR	
		HSP90AA1	
		HSP90AB1	
		HUWE1	
		LAMA1	
		LAMA5	
		MACF1	
		MAP1A	
		MAP2K3	
		MAP2K6	
		MAP3K10	
		MAP3K4	
		MAP4K4	
		MAPK8	
		MAPK9	
		MDN1	
		MGAM	
		MGMT	
		MLH3	
		MSH3	
		MSH5	
		MST1L	
		MXRA5	
		MYB	
		NBEAL2	
		NBPF1	
		NCOA3	
		NCOR2	
		NEB	
		NR1H2	
		PARP2	
		PARP3	
		PAXIP1	
		PCNXL2	
		PGR	
		PLEC	
		PLK1	
		PLXNA4	
		POLB	
		POLD1	

		POLH	
		POLQ	
		PRKCA	
		PRKCB	
		PRKCD	
		PRKCG	
		PRKD1	
		PTK2	
		RAD54B	
		RBBP8	
		RELN	
		RIF1	
		RPGR	
		RPS6KB1	
		SAAL1	
		SHC1	
		SHROOM4	
		SOS1	
		SPRY1	
		SPTA1	
		SRCAP	
		STAT1	
		STAT3	
		SVEP1	
		TBL1XR1	
		TENM1	
		TGFBR3	
		TOP2A	
		TP53BP1	
		TYK2	
		UBR4	
		USP36	
		WDFY3	
		XBP1	
		XPA	
		XPC	
		XRCC1	
		XRCC2	
		XRCC3	
		ZFHX3	
		ZFHX4	

		ZFP36L1	
		ZNF384	
		ZNF703	

Articles

Annals of Oncology 25: 1729–1735, 2014
doi:10.1093/annonc/mdu239
Published online 9 July 2014

Capturing intra-tumor genetic heterogeneity by *de novo* mutation profiling of circulating cell-free tumor DNA: a proof-of-principle

L. De Mattos-Arruda[1,2,3], B. Weigelt[3], J. Cortes[1], H. H. Won[3], C. K. Y. Ng[3], P. Nuciforo[1], F.-C. Bidard[3,4], C. Aura[1], C. Saura[1], V. Peg[5], S. Piscuoglio[3], M. Oliveira[1], Y. Smolders[3], P. Patel[6], L. Norton[7], J. Tabernero[1,2], M. F. Berger[3,†], J. Seoane[1,2,8,†] & J. S. Reis-Filho[3*,†]

[1]*Vall d'Hebron Institute of Oncology, Vall d'Hebron University Hospital, Barcelona;* [2]*Universitat Autònoma de Barcelona, Barcelona, Spain;* [3]*Department of Pathology, Memorial Sloan-Kettering Cancer Center, New York, USA;* [4]*Department of Medical Oncology, Institut Curie, Paris, France;* [5]*Department of Pathology, Vall d'Hebron University Hospital, Barcelona, Spain;* [6]*Genentech, Inc., San Francisco;* [7]*Department of Medicine, Memorial Sloan Kettering Cancer Center, New York, USA;* [8]*Institució Catalana de Recerca i Estudis Avançats (ICREA), Barcelona, Spain*

Received 9 June 2014; revised 20 June 2014; accepted 27 June 2014

Background: Plasma-derived cell-free tumor DNA (ctDNA) constitutes a potential surrogate for tumor DNA obtained from tissue biopsies. We posit that massively parallel sequencing (MPS) analysis of ctDNA may help define the repertoire of mutations in breast cancer and monitor tumor somatic alterations during the course of targeted therapy.

Patient and methods: A 66-year-old patient presented with synchronous estrogen receptor-positive/HER2-negative, highly proliferative, grade 2, mixed invasive ductal–lobular carcinoma with bone and liver metastases at diagnosis. DNA extracted from archival tumor material, plasma and peripheral blood leukocytes was subjected to targeted MPS using a platform comprising 300 cancer genes known to harbor actionable mutations. Multiple plasma samples were collected during the fourth line of treatment with an AKT inhibitor.

Results: Average read depths of 287x were obtained from the archival primary tumor, 139x from the liver metastasis and between 200x and 900x from ctDNA samples. Sixteen somatic non-synonymous mutations were detected in the liver metastasis, of which 9 (*CDKN2A*, *AKT1*, *TP53*, *JAK3*, *TSC1*, *NF1*, *CDH1*, *MML3* and *CTNNB1*) were also detected in >5% of the alleles found in the primary tumor sample. Not all mutations identified in the metastasis were reliably identified in the primary tumor (e.g. *FLT4*). Analysis of ctDNA, nevertheless, captured all mutations present in the primary tumor and/or liver metastasis. In the longitudinal monitoring of the patient, the mutant allele fractions identified in ctDNA samples varied over time and mirrored the pharmacodynamic response to the targeted therapy as assessed by positron emission tomography–computed tomography.

Conclusions: This proof-of-principle study is one of the first to demonstrate that high-depth targeted MPS of plasma-derived ctDNA constitutes a potential tool for *de novo* mutation identification and monitoring of somatic genetic alterations during the course of targeted therapy, and may be employed to overcome the challenges posed by intra-tumor genetic heterogeneity.

Registered clinical trial: www.clinicaltrials.gov, NCT01090960.

Key words: massively parallel sequencing, breast cancer, cell-free tumor DNA, intra-tumor heterogeneity, disease monitoring

introduction

Massively parallel sequencing (MPS) studies have revealed that cancers are characterized by remarkable genetic complexity, and that intra-tumor genetic heterogeneity is not an uncommon phenomenon [1–6]. The spatial and temporal intra-tumor genetic heterogeneity documented in breast cancers [4, 5, 7, 8] may have important implications for biomarker discovery programs and targeted cancer therapeutics [9, 10].

Given the spatial and temporal heterogeneity documented between primary cancers and metastatic lesions [2, 11], primary tumor biopsies may not constitute an ideal source for the genetic characterization of metastatic disease and extensive

*Correspondence to: Dr Jorge S. Reis-Filho, Department of Pathology, Memorial Sloan-Kettering Cancer Center, 1275 York Avenue, New York, NY 10065, USA. Tel: +1-212-639-8054; Fax: +1-212-639-2502; E-mail: reisfilj@mskcc.org

†MFB, JS and JSR-F contributed equally to this work.

sampling of metastatic deposits is often unfeasible [2, 6, 9, 10]. Hence, approaches that provide a global assessment of the constellation of somatic genetic alterations in a cancer irrespective of its anatomical location would be required for the identification of potential therapeutic targets and mechanisms of resistance, in particular in the context of patients with metastatic disease.

Minimally invasive approaches that may help overcome the challenges posed by intra-tumor spatial and temporal heterogeneity and by the sampling bias stemming from the analysis of single-tumor biopsies have been developed [10, 12–15]. Plasma-derived cell-free tumor DNA (ctDNA) has been tested as a potential non-invasive surrogate for tumor tissue biopsies [10]. Given that ctDNA is believed to be shed into the circulation by cancer cells from both the primary tumor and/or its metastases, it may constitute a source of tumor material from all disease sites, offering a real time, easily obtainable and minimally invasive tool for the development of molecular biomarkers [9, 10].

Recent studies have shown that somatic genetic alterations can be identified by MPS-based analysis of ctDNA from plasma of breast cancer patients [13–18]. Thus, the genomic characterization of plasma ctDNA has introduced new means to investigate the metastatic process and mechanisms of therapeutic resistance, and to monitor actionable driver somatic genomic alterations during the course of therapy in breast cancer patients [9, 13–15, 17, 19, 20].

We hypothesize that MPS analysis of plasma-derived ctDNA of breast cancer patients would constitute a means to identify and monitor the presence of potentially actionable driver somatic genomic alterations during the course of therapy. In this proof-of-concept study, we demonstrate that MPS analysis of plasma-derived ctDNA resulted in the identification of the complete repertoire of mutations detected in the metastatic lesion, and that changes in mutant allele fractions (MAFs) in ctDNA mirrored the pharmacodynamic response to targeted monotherapy.

patient and methods

patient

A 66-year-old, postmenopausal woman was diagnosed with an estrogen receptor (ER)-positive/HER2-negative, grade 2, mixed invasive ductal–lobular carcinoma of the breast and synchronous bone and liver metastases at Vall d'Hebron University Hospital (Barcelona, Spain) in July 2010. Imaging-guided biopsies of the primary tumor and liver metastasis were obtained before the initiation of systemic therapy. Following three lines of chemotherapy (i.e. paclitaxel-, anthracycline- and capecitabine-based therapies; Figure 1) and disease progression, the patient underwent a molecular pre-screening program in November 2011. The analysis of archival primary breast tumor material by Sequenom MassARRAY® revealed the presence of an *AKT1* E17K mutation, with an MAF of 88% (supplementary Table S1, available at *Annals of Oncology* online). Based on these results, the patient was enrolled in the phase I study PAM4743g (Clinicaltrials.gov, NCT01090960) in January 2012 and treated with Ipatasertib (GDC-0068), a highly selective, orally available pan-AKT inhibitor [21] as the fourth line of therapy. A dose of 600 mg once daily (maximum tolerated dose in the expansion cohort was 400 mg) was administered on a 3-week-on/1-week-off treatment schedule, until documented disease progression in September 2012. Plasma samples were collected at baseline (i.e. before therapy), and during the treatment with Ipatasertib at 2 months, 6 months and at the time of disease progression. Response was assessed using the RECIST criteria (1.1) [22]. This study was approved by the IRB of Vall d'Hebron University Hospital.

DNA extraction

The diagnosis of the primary breast tumor and synchronous liver metastasis was confirmed by histologic review (supplementary Figure S1, available at *Annals of Oncology* online). Five 10-μm thick formalin-fixed paraffin-embedded (FFPE) sections of the primary breast tumor and liver metastasis were microdissected with a needle under a stereomicroscope to ensure >80% of tumor cell content, as previously described [23]. DNA from tumor samples was extracted using the RecoverAll™ Total Nucleic Acid Isolation Kit (Ambion, Austin, TX) for FFPE tissue, and germline DNA was extracted from peripheral blood leukocytes using the QIAamp DNA Blood Mini Kit (Qiagen, Valencia, CA), according to the manufacturers' instructions. Plasma-derived DNA was extracted with the QIAamp Circulating Nucleic Acid Kit (Qiagen), as per the manufacturer's protocol. DNA was quantified using the Qubit Fluorometer (Invitrogen, Life Technologies, Grand Island, NY).

targeted massively parallel sequencing

DNA samples from the primary breast cancer, liver metastasis, and from multiple plasma samples as well as germline DNA obtained from peripheral blood leukocytes were subjected to targeted capture MPS at the Integrated Genomics Operation (iGO), Memorial Sloan Kettering Cancer Center using the Integrated Mutation Profiling of Actionable Cancer Targets (IMPACT) platform [24], which comprises 300 cancer genes known to harbor actionable mutations as previously described (supplementary Table S2, available at *Annals of Oncology* online) [3]. In brief, barcoded sequence libraries were prepared (New England Biolabs, KapaBiosystems) using 22–250 ng of input DNA, pooled and captured using oligonucleotides for all protein-coding exons of the 300 genes (NimblegenSeqCap) [3]. Sequencing was carried out on an Illumina HiSeq2000 (San Diego, CA). Sequence alignment as well as calling of somatic single-nucleotide variants and small insertions and deletions were carried out as previously described [3, 24]. All candidate mutations were reviewed manually using the Integrative Genomics Viewer [25]. Mutations with an allele fraction of <1% and/or supported by ≤2 reads were disregarded.

Sequenom analysis

As a molecular pre-screening tool to select patients for clinical trials, 600 ng of DNA from the primary tumor was subjected to mutation profiling using a customized version of the OncoCarta Panel v1.0 (Sequenom MassARRAY®, San Diego, CA) (supplementary Table S1, available at *Annals of Oncology* online). Data analyses and mutation reports were generated using the Sequenom® software.

results

High-depth targeted MPS was carried out with DNA obtained from the ER-positive/HER2-negative primary breast cancer and synchronous liver metastasis sampled at the time of diagnosis, and multiple plasma samples collected during the fourth line of therapy with Ipatasertib. Ipatasertib monotherapy provided benefit in terms of long-lasting radiologic and biochemical responses as shown by CA15.3 levels (Figure 2), and stable disease as per RECIST 1.1 was the best response achieved by the patient and lasted for ∼8 months. We subsequently compared the patient's progression-free survival (PFS) on Ipatasertib (A) with the PFS for the most recent therapy on which the patient had experienced

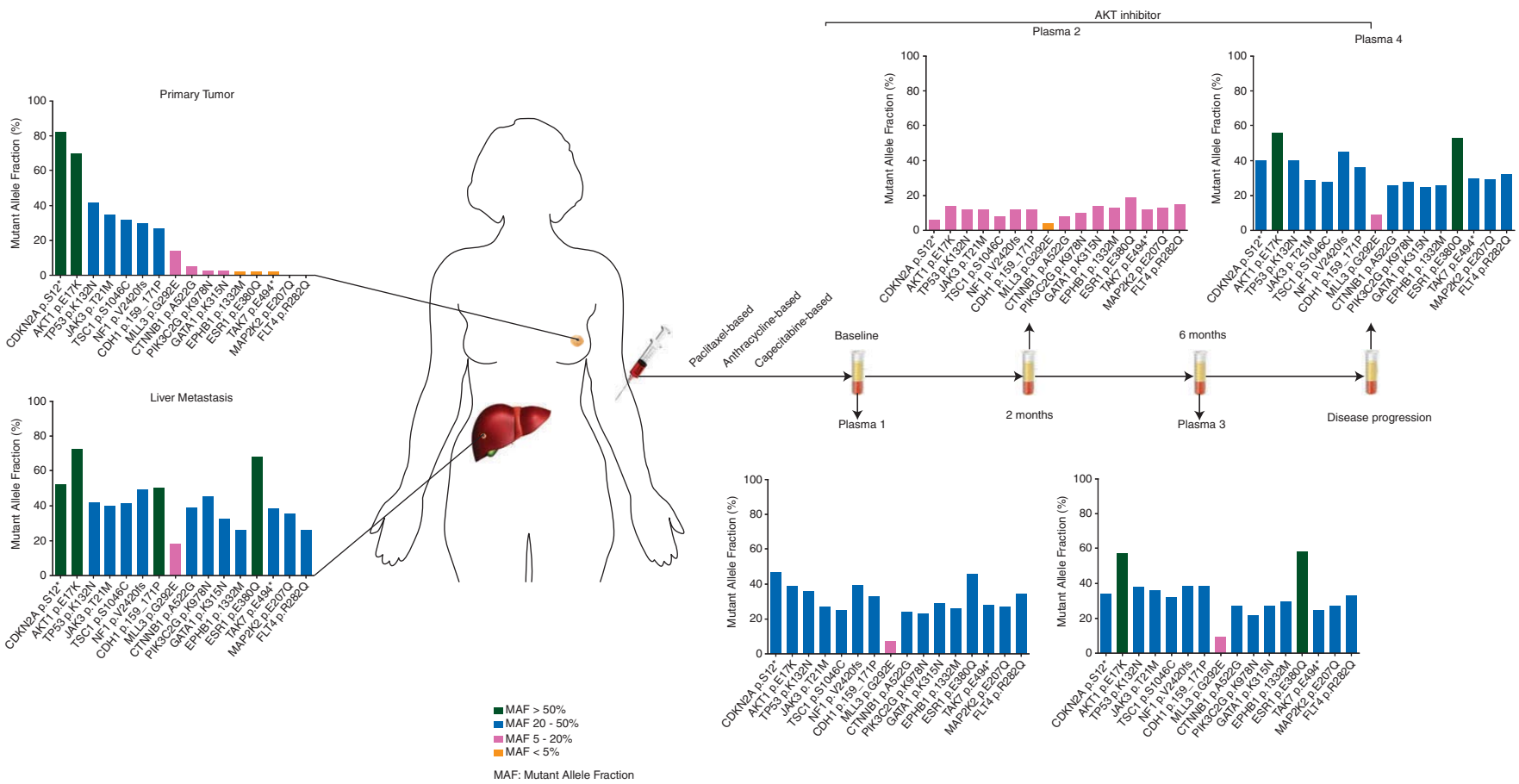

Figure 1. Patient disease presentation, treatment timeline and mutant alleles in the primary breast tumor, liver metastasis and plasma-derived DNA. Biopsies of the primary breast cancer and its synchronous liver metastasis were obtained before initiation of therapy. Following three lines of chemotherapy, the patient was treated with the AKT inhibitor Ipatasertib, and multiple plasma samples were obtained during the course of treatment. DNA samples extracted from the primary tumor, metastasis and plasma samples were subjected to targeted high-depth massively parallel sequencing. Not all mutations identified in the metastasis were reliably identified in the primary breast tumor; however, all mutations present in the primary tumor and/or liver metastasis were found in ctDNA.

doi:10.1093/annonc/mdu239 | 1731

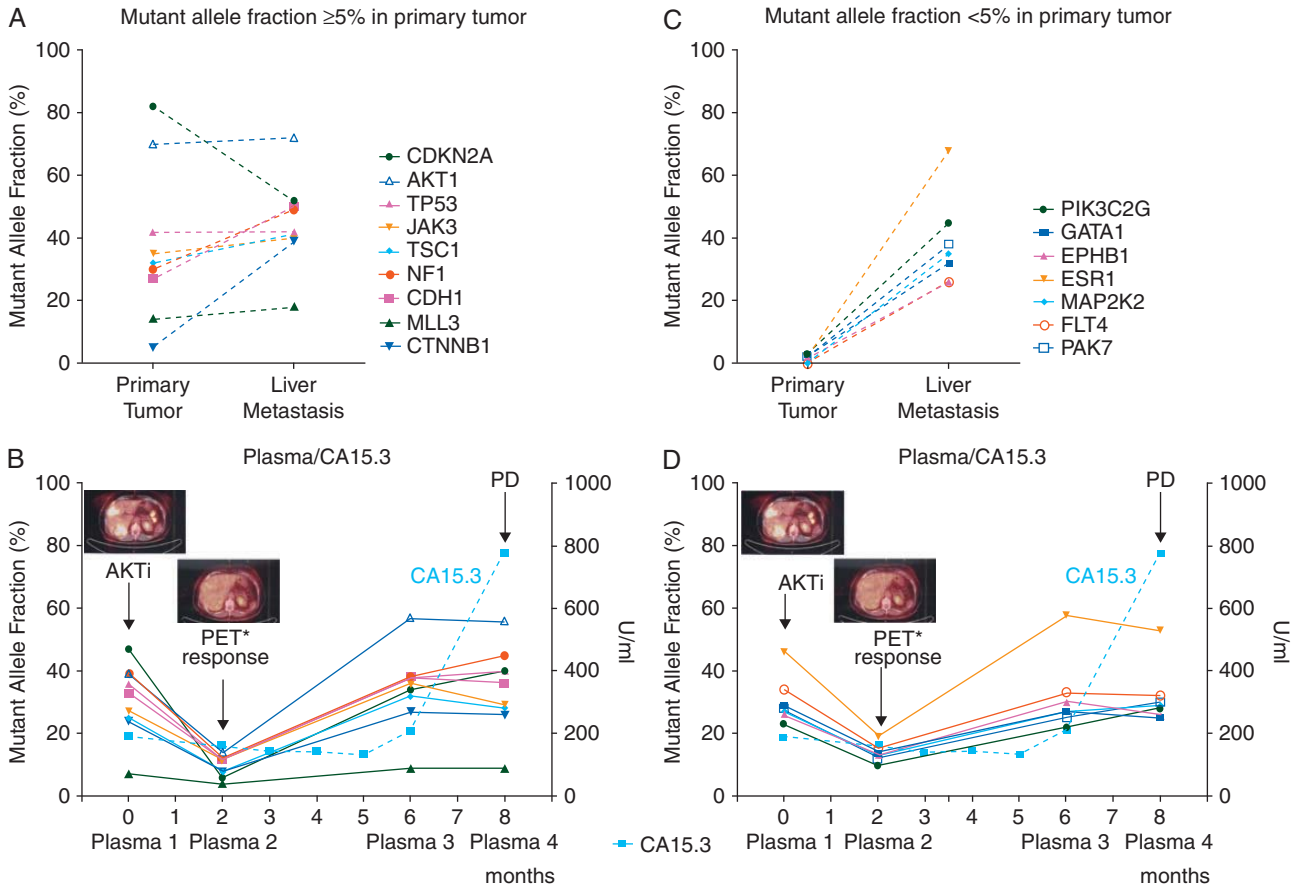

Figure 2. Representation of the mutant alleles in the primary tumor and metastasis and longitudinal monitoring of CA15.3 levels in four plasma-derived ctDNA samples. Genes whose high confidence mutations were detected at a mutant allele fraction (MAF) of ≥5% in the primary tumor are depicted in (A) and (B), whereas genes whose high confidence mutations were detected in the plasma-derived ctDNA, but either absent or present at a MAF of <5% in the primary tumor, are illustrated in (C) and (D). In (B) and (D), representative PET–CT images obtained at baseline and 2 months after initiation of Ipatasertib monotherapy; CA15.3 levels assessed during the fourth line of systemic treatment with Ipatasertib monotherapy. Arrow, initiation of Ipatasertib (AKTi) monotherapy. PD, progressive disease; *PET–CT, pharmacodynamic response.

progression (i.e. capecitabine-based) (B) [26]. The ratio of the PFS of period B/PFS of period A was 3.1 (i.e. 7.8 months/2.5 months), superior to a ratio of >1.3, corroborating the potential clinical benefit of Ipatasertib monotherapy for this patient [26].

somatic genetic alterations are distinct between the primary tumor and its metastasis

Targeted capture MPS showed average read depths of 287x and 139x in the archival primary breast cancer and its liver metastasis, respectively, and 76x in the normal sample. Fifteen somatic non-synonymous mutations were detected in the primary tumor (*CDKN2A*, *AKT1*, *TP53*, *JAK3*, *TSC1*, *NF1*, *CDH1*, *MLL3*, *CTNNB1*, *PIK3C2G*, *GATA1*, *EPHB1*, *ESR1* and *PAK7*), all of which were also detected in the liver metastasis (Table 1). Mutations affecting *FLT4* and *MAP2K2* were present in the liver metastasis (present in 12/47 reads and 40/113 reads, respectively), but could not be reliably detected in the primary tumor (found in 2/89 reads and 2/137 reads, respectively).

Analysis of the primary tumor and its liver metastasis revealed similar MAFs of the *AKT1* (70% and 72% in the primary tumor and its metastasis, respectively) and *TP53* (42% in the primary tumor and its metastasis) somatic mutations present in these samples (Table 1). On the basis of the allele fractions of the mutations affecting these two genes, it would be reasonable to hypothesize that these mutations were clonally distributed in the cancer cells of both the primary tumor and its liver metastasis. Evidence of intra-tumor genetic heterogeneity was, however, observed, given that the liver metastasis was enriched for mutations either only present at low allele fractions in the primary tumor (i.e. <5% MAF; *PIK3C2G*, *GATA1*, *EPHB1*, *ESR1* and *PAK7*) or found at a MAF beyond the resolution obtained with the sequencing depth achieved for the primary tumor sample (i.e. *FLT4* and *MAP2K2* mutations; Table 1 and Figure 2). Targeted capture MPS also confirmed the presence of the *AKT1* E17K mutation identified by Sequenom MassARRAY® during the molecular pre-screening program at Vall d'Hebron University Hospital (Table 1 and supplementary Table S1, available at *Annals of Oncology* online).

ctDNA analysis captures the heterogeneity of primary tumor and metastasis

Targeted capture MPS of the multiple plasma-derived DNA samples yielded average read depths ranging from 209x to 918x. Importantly, MAFs of up to 57% and 58% for *AKT1* E17K and

Table 1. Allele fractions of somatic mutations identified in the primary breast tumor, liver metastasis and plasma samples

Gene	Mutation (amino acid)	Primary tumor (287x) MAFs (reads)	Liver metastasis (139x) MAFs (reads)	Plasma 1 (692x) MAFs (reads)	Plasma 2 (728x) MAFs (reads)	Plasma 3 (209x) MAFs (reads)	Plasma 4 (918x) MAFs (reads)
CDKN2A	p.S12*	82% (23/28)	52% (11/21)	47% (42/89)	6% (7/117)	34% (14/41)	40% (55/137)
AKT1	p.E17K	70% (83/118)	72% (79/110)	39% (204/521)	14% (83/593)	57% (100/174)	56% (373/663)
TP53	p.K132N	42% (101/241)	42% (48/113)	36% (228/625)	12% (92/753)	38% (78/204)	40% (339/841)
JAK3	p.T21M	35% (60/172)	40% (56/141)	27% (253/939)	12% (100/834)	36% (122/340)	29% (343/1181)
TSC1	p.S1046C	32% (31/98)	41% (55/134)	25% (132/521)	8% (43/518)	32% (59/182)	28% (179/636)
NF1	p.V2420fs	30% (153/511)	49% (61/124)	39% (186/483)	12% (92/761)	38% (49/159)	45% (328/726)
CDH1	p.159_171 PPISCPENEKGPF>L	27% (56/210)	50% (46/92)	33% (197/605)	12% (93/758)	38% (52/138)	36% (265/731)
MLL3	p.G292E	14% (64/446)	18% (30/168)	7% (67/1002)	4% (48/1183)	9% (31/352)	9% (73/831)
CTNNB1	p.A522G	5% (12/256)	39% (60/155)	24% (130/551)	8% (47/618)	27% (54/198)	26% (164/641)
PIK3C2G	p.K978N	3% (16/492)	45% (113/250)	23% (176/752)	10% (80/803)	22% (44/200)	28% (268/960)
GATA1	p.K315N	3% (5/192)	32% (35/111)	29% (313/1071)	14% (154/1067)	27% (100/370)	25% (419/1648)
EPHB1	p.I332M	2% (5/211)	26% (25/96)	26% (261/1015)	13% (120/919)	30% (102/343)	26% (348/1322)
ESR1	p.E380Q	2% (7/287)	68% (106/157)	46% (339/737)	19% (158/823)	58% (160/275)	53% (534/1009)
PAK7	p.E494*	2% (5/304)	38% (56/148)	28% (202/715)	12% (83/701)	25% (55/224)	30% (273/897)
MAP2K2	p.E207Q	NRD (2/137)	35% (40/113)	27% (221/815)	13% (106/823)	27% (72/270)	29% (309/1076)
FLT4	p.R282Q	NRD (2/89)	26% (12/47)	34% (225/667)	15% (98/638)	33% (89/270)	32% (266/820)

Color coding: dark gray cells, MAF > 50%; light gray cells, MAF 20%–50%; pale gray cells, MAF 5%–20% and white cells, MAF < 5% or no mutation identified (NRD, not reliably detected). All mutations detected in both the primary breast tumor and synchronous liver metastasis could be identified in the multiple plasma samples. Plasma 1, baseline; plasma 2, 2 months after initiation of AKT inhibitor Ipatasertib treatment; plasma 3, 6 months after initiation AKT inhibitor Ipatasertib treatment; plasma 4, at disease progression.

*, stop codon.

MAF, mutant allele fraction.

ESR1 E380Q were detected in the plasma DNA, respectively, providing evidence to suggest that most of the cell-free plasma DNA obtained from this patient was tumor-derived.

Interestingly, while not all mutations identified in the liver metastasis could accurately be detected in the primary tumor at the sequencing depth obtained, sequencing analysis of ctDNA from this patient captured the entire repertoire of mutations found in the primary tumor and/or metastatic deposit (Figures 1 and 2, and Table 1). For instance, a missense mutation in *FLT4*, present in the metastasis but found at a MAF beyond the resolution of targeted MPS of the primary tumor material, was captured in the plasma-derived ctDNA. All 16 mutations except *MLL3* were found in the baseline plasma ctDNA sample with allelic fractions of >20% (Table 1). The presence of the *AKT1* E17K mutation in the plasma samples 1 and 2 was validated independently by means of Sequenom MassARRAY® analysis (44% and 16% MAFs, respectively; supplementary Table S1, available at *Annals of Oncology* online). Further validation of the somatic genetic aberrations was not possible, given that no additional biological material was available for the remaining samples.

plasma-derived ctDNA for longitudinal disease monitoring

In the longitudinal monitoring of the patient during the course of Ipatasertib treatment, the MAFs identified in ctDNA samples varied following the administration of the targeted therapy. Two months after the initiation of the treatment (plasma 2), the fraction of all mutant alleles detected in the plasma-derived ctDNA decreased when compared with ctDNA analysis at baseline (plasma 1), mirroring the pharmacodynamic response as assessed by PET–CT (Figure 2). Assessment of ctDNA at 6 months of treatment (plasma 3) revealed an increase in the MAFs of all mutated genes similar to the levels observed at baseline before treatment (Figure 2 and Table 1). It should be noted, however, that the MAFs of *AKT1* and *ESR1* were increased in the ctDNA at 6 months when compared with baseline (*AKT1* E17K 39% plasma 1 versus 57% plasma 3; *ESR1* E380Q 46% plasma 1 versus 58% plasma 3; Figure 2 and Table 1). Furthermore, the increase in mutant alleles in plasma-derived ctDNA was observed before radiologic disease progression (data not shown), and before the increase in CA15.3 levels (Figure 2), providing evidence to suggest that increases in disease burden can be detected earlier by ctDNA analysis than by classical biochemical and radiologic assessments.

discussion

Here we demonstrate that high-depth targeted MPS of plasma-derived ctDNA contains representative tumor-derived genetic material that captured all mutations detected in the primary tumor and/or its synchronous liver metastasis, and provide a proof-of-principle that this approach can potentially be employed as a quantitative marker for disease monitoring of somatic genetic alterations during the course of targeted therapy.

At the time of diagnosis, at least a subset of breast cancers have been shown to constitute mosaics, being composed of heterogeneous populations of tumor cells that, in addition to the founder genetic events, harbor private mutations [4–8]. Consistent with this notion, here we demonstrate that mutations affecting *ESR1*, *CTNNB1*, *PIK3C2G*, *GATA1*, *EPHB1*, *PAK7*, *MAP2K2* and *FLT4*, albeit present at allele fractions ≥26% in the metastatic lesion, were likely present in a minor clone of the primary tumor (i.e. MAFs ≤5%). It should be noted that activating *ESR1* mutations have been identified in endocrine-resistant metastatic lesions while not detectable in the respective primary breast cancers [27]. In this study, the endocrine therapy resistance-associated *ESR1* E380Q mutation [28] was present at a higher allele fraction in the ER-positive liver metastasis (MAF 68%) than in its synchronous ER-positive primary breast cancer (MAF 2%). Importantly, however, the biopsies of the synchronous primary and metastatic lesions were collected before any systemic therapy. It remains to be determined whether the *ESR1* E380Q mutation provided a growth advantage at the metastatic site irrespective of treatment or merely co-segregated with other molecular alterations present in the clone that gave rise to the metastatic deposit.

Spatial and temporal intra-tumor genetic heterogeneity has been documented in cancers [2, 5–8, 11, 29], suggesting that genetic analysis of a single diagnostic biopsy of a primary tumor may not yield results that are representative of the somatic genetic aberrations present in the cancer cells of its metastases [2, 30]. Given that in the present case all mutations detectable by targeted MPS of the metastatic lesion were also detected in the plasma ctDNA samples, our findings lend credence to the notion that ctDNA may constitute an alternative to metastatic lesion sampling for MPS analysis.

Our study has several limitations. First, the analyses were carried out utilizing materials from a single patient with a high disease burden. The high MAFs observed in this study likely reflect this high tumor burden the patient presented, and therefore, an ideal setting for plasma DNA analysis. It is plausible that, in other settings and cancer types, this approach may not be sufficient, either due to lower tumor burden or due to the fact that cancer cells may not harbor mutations in any of the genes included in a given targeted capture panel [9]. In fact, in Bettegowda et al. [15], the vast majority of metastatic breast cancer patients had ctDNA detectable in plasma, whereas <50% of breast cancer patients with early disease had any detectable levels of ctDNA. Secondly, although ctDNA-targeted capture analysis was proven useful for disease monitoring, sequencing analysis of the plasma DNA sample at progression did not result in the identification of a genetic aberration causative of resistance to Ipatasertib monotherapy. Although resistance to AKT inhibition may be mediated by adaptive changes (e.g. activation of upstream receptor tyrosine kinases [31]), it is unknown whether this mechanism would induce resistance to the Ipatasertib monotherapy in patients harboring *AKT1* mutations. Thirdly, given that all mutations found in the primary tumor were also detected in the liver metastasis, we cannot ascertain whether ctDNA not only capture the entire repertoire of mutations found in the metastatic lesion, but also that of the primary tumor. Regrettably, the amounts of plasma DNA obtained from this patient were insufficient for whole genome or whole exome sequencing analysis at the depth that would be required to determine whether a specific somatic genetic aberration was selected for during Ipatasertib monotherapy and to define whether there would be mutations affecting genes not included in the IMPACT assay that would be present in the primary tumor but not in the metastatic lesion.

In conclusion, we have demonstrated that plasma-derived DNA contains representative tumor genetic material that may be employed to uncover somatic genetic alterations present in cancer cells from patients with metastatic disease. Targeted capture MPS analysis of ctDNA may be a tool to combat intra-tumor genetic heterogeneity and to monitor tumor somatic alterations during the course of targeted therapy.

acknowledgements

The authors thank A. Vivancos for the Sequenom data.

funding

LDM-A was supported in part by a Translational Research grant from the European Society for Medical Oncology (ESMO Translational Research Fellowship). The authors acknowledge Fundación Rafael del Pino for financial support (for LDMA and JT) and Asociación Española contra el Cáncer and the Steiner Foundation (for JS). No grant numbers apply.

disclosure

PP is an employee of Genentech/Roche. The other authors have no conflicts of interest.

references

1. Swanton C. Intratumor heterogeneity: evolution through space and time. Cancer Res 2012; 72: 4875–4882.
2. Gerlinger M, Rowan AJ, Horswell S et al. Intratumor heterogeneity and branched evolution revealed by multiregion sequencing. N Engl J Med 2012; 366: 883–892.
3. De Mattos-Arruda L, Bidard FC, Won HH et al. Establishing the origin of metastatic deposits in the setting of multiple primary malignancies: the role of massively parallel sequencing. Mol Oncol 2014; 8: 150–158.
4. Shah SP, Roth A, Goya R et al. The clonal and mutational evolution spectrum of primary triple-negative breast cancers. Nature 2012; 486: 395–399.
5. Nik-Zainal S, Van Loo P, Wedge DC et al. The life history of 21 breast cancers. Cell 2012; 149: 994–1007.
6. Martelotto LG, Ng CK, Piscuoglio S et al. Breast cancer intra-tumor heterogeneity. Breast Cancer Res 2014; 16: 210.
7. Geyer FC, Weigelt B, Natrajan R et al. Molecular analysis reveals a genetic basis for the phenotypic diversity of metaplastic breast carcinomas. J Pathol 2010; 220: 562–573.
8. Navin N, Kendall J, Troge J et al. Tumour evolution inferred by single-cell sequencing. Nature 2011; 472: 90–94.
9. Bidard FC, Weigelt B, Reis-Filho JS. Going with the flow: from circulating tumor cells to DNA. Sci Transl Med 2013; 5: 207ps214.
10. De Mattos-Arruda L, Cortes J, Santarpia L et al. Circulating tumour cells and cell-free DNA as tools for managing breast cancer. Nat Rev Clin Oncol 2013; 10: 377–389.
11. Yap TA, Gerlinger M, Futreal PA et al. Intratumor heterogeneity: seeing the wood for the trees. Sci Transl Med 2012; 4: 127ps110.
12. Powell AA, Talasaz AH, Zhang H et al. Single cell profiling of circulating tumor cells: transcriptional heterogeneity and diversity from breast cancer cell lines. PLoS ONE 2012; 7: e33788.

13. Forshew T, Murtaza M, Parkinson C et al. Noninvasive identification and monitoring of cancer mutations by targeted deep sequencing of plasma DNA. Sci Transl Med 2012; 4: 136ra168.
14. Dawson SJ, Rosenfeld N, Caldas C. Circulating tumor DNA to monitor metastatic breast cancer. N Engl J Med 2013; 369: 93–94.
15. Bettegowda C, Sausen M, Leary RJ et al. Detection of circulating tumor DNA in early- and late-stage human malignancies. Sci Transl Med 2014; 6: 224ra224.
16. Leary RJ, Sausen M, Kinde I et al. Detection of chromosomal alterations in the circulation of cancer patients with whole-genome sequencing. Sci Transl Med 2012; 4: 162ra154.
17. Murtaza M, Dawson SJ, Tsui DW et al. Non-invasive analysis of acquired resistance to cancer therapy by sequencing of plasma DNA. Nature 2013; 497: 108–112.
18. Chan KC, Jiang P, Zheng YW et al. Cancer genome scanning in plasma: detection of tumor-associated copy number aberrations, single-nucleotide variants, and tumoral heterogeneity by massively parallel sequencing. Clin Chem 2013; 59: 211–224.
19. Misale S, Yaeger R, Hobor S et al. Emergence of KRAS mutations and acquired resistance to anti-EGFR therapy in colorectal cancer. Nature 2012; 486: 532–536.
20. Zhang L, Ridgway LD, Wetzel MD et al. The identification and characterization of breast cancer CTCs competent for brain metastasis. Sci Transl Med 2013; 5: 180ra148.
21. Lin J, Sampath D, Nannini MA et al. Targeting activated Akt with GDC-0068, a novel selective Akt inhibitor that is efficacious in multiple tumor models. Clin Cancer Res 2013; 19: 1760–1772.
22. Eisenhauer EA, Therasse P, Bogaerts J et al. New response evaluation criteria in solid tumours: revised RECIST guideline (version 1.1). Eur J Cancer 2009; 45: 228–247.
23. Hernandez L, Wilkerson PM, Lambros MB et al. Genomic and mutational profiling of ductal carcinomas in situ and matched adjacent invasive breast cancers reveals intra-tumour genetic heterogeneity and clonal selection. J Pathol 2012; 227: 42–52.
24. Won HH, Scott SN, Brannon AR et al. Detecting somatic genetic alterations in tumor specimens by exon capture and massively parallel sequencing. J Vis Exp 2013; 80: e50710.
25. Robinson JT, Thorvaldsdottir H, Winckler W et al. Integrative genomics viewer. Nat Biotechnol 2011; 29: 24–26.
26. Von Hoff DD, Stephenson JJ, Jr, Rosen P et al. Pilot study using molecular profiling of patients' tumors to find potential targets and select treatments for their refractory cancers. J Clin Oncol 2010; 28: 4877–4883.
27. Polyak K. Tumor heterogeneity confounds and illuminates: a case for Darwinian tumor evolution. Nat Med 2014; 20: 344–346.
28. Li S, Shen D, Shao J et al. Endocrine-therapy-resistant ESR1 variants revealed by genomic characterization of breast-cancer-derived xenografts. Cell Rep 2013; 4: 1116–1130.
29. Gerlinger M, Horswell S, Larkin J et al. Genomic architecture and evolution of clear cell renal cell carcinomas defined by multiregion sequencing. Nat Genet 2014; 46: 225–233.
30. Sottoriva A, Spiteri I, Piccirillo SG et al. Intratumor heterogeneity in human glioblastoma reflects cancer evolutionary dynamics. Proc Natl Acad Sci USA 2013; 110: 4009–4014.
31. Chandarlapaty S, Sawai A, Scaltriti M et al. AKT inhibition relieves feedback suppression of receptor tyrosine kinase expression and activity. Cancer Cell 2011; 19: 58–71.

Annals of Oncology 25: 1735–1742, 2014
doi:10.1093/annonc/mdu211
Published online 6 June 2014

Final report of the phase I/II clinical trial of the E75 (nelipepimut-S) vaccine with booster inoculations to prevent disease recurrence in high-risk breast cancer patients

E. A. Mittendorf[1], G. T. Clifton[2], J. P. Holmes[3], E. Schneble[4], D. van Echo[5], S. Ponniah[6] & G. E. Peoples[4,6]*

[1]Department of Surgical Oncology, The University of Texas MD Anderson Cancer Center, Houston; [2]Blanchfield Army Community Hospital, Fort Campbell; [3]Redwood Regional Medical Group, Santa Rosa; [4]Department of Surgery, Brooke Army Medical Center, Ft Sam Houston; [5]Department of Hematology Oncology, Walter Reed Army Medical Center, Washington; [6]Department of Surgery, Cancer Vaccine Development Program, United States Military Cancer Institute, Uniformed Services University of the Health Sciences, Bethesda, USA

Received 22 March 2014; revised 24 May 2014; accepted 27 May 2014

Background: E75 (nelipepimut-S) is a human leukocyte antigen (HLA)-A2/A3-restricted immunogenic peptide derived from the HER2 protein. We have conducted phase I/II clinical trials vaccinating breast cancer patients with nelipepimut-S and granulocyte–macrophage colony-stimulating factor (GM-CSF) in the adjuvant setting to prevent disease recurrence. All patients have completed 60 months follow-up, and here, we report the final analyses.

*Correspondence to: Dr George E. Peoples, Department of Surgery, Brooke Army Medical Center, 3851 Roger Brooke Drive, Ft Sam Houston, TX, USA. Tel: +1-210-916-1117; E-mail: george.peoples@us.army.mil

nature COMMUNICATIONS

ARTICLE

Received 25 Mar 2015 | Accepted 8 Oct 2015 | Published 10 Nov 2015

DOI: 10.1038/ncomms9839 OPEN

Cerebrospinal fluid-derived circulating tumour DNA better represents the genomic alterations of brain tumours than plasma

Leticia De Mattos-Arruda[1,2,3], Regina Mayor[1], Charlotte K.Y. Ng[2], Britta Weigelt[2], Francisco Martínez-Ricarte[3,4], Davis Torrejon[1], Mafalda Oliveira[1], Alexandra Arias[1], Carolina Raventos[1], Jiabin Tang[5], Elena Guerini-Rocco[2], Elena Martínez-Sáez[4], Sergio Lois[4], Oscar Marín[4], Xavier de la Cruz[4,6], Salvatore Piscuoglio[2], Russel Towers[7], Ana Vivancos[1], Vicente Peg[4], Santiago Ramon y Cajal[3,4], Joan Carles[1], Jordi Rodon[1], María González-Cao[8], Josep Tabernero[1,3], Enriqueta Felip[1,3], Joan Sahuquillo[3,4], Michael F. Berger[5,9], Javier Cortes[1,3], Jorge S. Reis-Filho[2] & Joan Seoane[1,3,6]

Cell-free circulating tumour DNA (ctDNA) in plasma has been shown to be informative of the genomic alterations present in tumours and has been used to monitor tumour progression and response to treatments. However, patients with brain tumours do not present with or present with low amounts of ctDNA in plasma precluding the genomic characterization of brain cancer through plasma ctDNA. Here we show that ctDNA derived from central nervous system tumours is more abundantly present in the cerebrospinal fluid (CSF) than in plasma. Massively parallel sequencing of CSF ctDNA more comprehensively characterizes the genomic alterations of brain tumours than plasma, allowing the identification of actionable brain tumour somatic mutations. We show that CSF ctDNA levels longitudinally fluctuate in time and follow the changes in brain tumour burden providing biomarkers to monitor brain malignancies. Moreover, CSF ctDNA is shown to facilitate and complement the diagnosis of leptomeningeal carcinomatosis.

[1] Vall d'Hebron Institute of Oncology, Vall d'Hebron University Hospital, P. Vall d'Hebron 119-129, 08035 Barcelona, Spain. [2] Department of Pathology, Memorial Sloan Kettering Cancer Center, 1275 York Avenue, New York, New York 10065, USA. [3] Universitat Autònoma de Barcelona, 08193 Barcelona, Spain. [4] Vall d'Hebron Institute of Research, Vall d'Hebron University Hospital, Ps Vall d'Hebron 119-129, 08035 Barcelona, Spain. [5] Center for Molecular Oncology, Memorial Sloan Kettering Cancer Center, 1275 York Avenue, New York, NY 10065, USA. [6] Institució Catalana de Recerca i Estudis Avançats (ICREA), Barcelona, Spain. [7] Department of Surgery, Memorial Sloan Kettering Cancer Center, 1275 York Avenue, New York, NY 10065, USA. [8] Quirón Dexeus University Hospital, 08028 Barcelona, Spain. [9] Human Oncology and Pathogenesis Program, Memorial Sloan Kettering Cancer Center, 1275 York Avenue, New York, NY 10065, USA. Correspondence and requests for materials should be addressed to J.S. (email: jseoane@vhio.net).

The genomic characterization of tumours is crucial for the optimal diagnosis and treatment of cancer. Given the reported spatial and temporal intratumour heterogeneity, repeated biopsies are required for an adequate characterization of the somatic genetic alterations found in human cancers[1,2]. This approach has important limitations, particularly in the case of brain malignancies[3], due to the restricted and invasive access for sampling tumour material and the challenges to recapitulate the tumour clonal diversity through the analysis of a small fragment of the tumour. Recent work has shown that cell-free circulating tumour DNA (ctDNA) in the plasma could be used to characterize and monitor tumours[4–7]. ctDNA analysis of patients with brain tumours, however, has revealed either absence or very low levels of tumour DNA in plasma[7].

The cerebrospinal fluid (CSF) is in intimate contact with tumour cells in central nervous system (CNS) cancers and, recently, ctDNA has been shown to be present in the CSF of patients with brain tumours[8,9]. The aim of our work was to determine whether the analysis of CSF ctDNA could be useful for the characterization and monitoring of brain tumours in comparison with plasma ctDNA. We applied hybridization capture-based massively parallel targeted sequencing and/or exome sequencing coupled with droplet digital PCR (ddPCR) to synchronous CSF and plasma-derived ctDNA, and tumour tissue deposits from patients with glioblastoma (GBM), medulloblastoma (Medullo), and brain metastases from lung cancer (BMLC) and from breast cancer (BMBC, six of them subjected to warm autopsies) including breast cancer patients with clinical features suggestive of leptomeningeal carcinomatosis (LC). In this study, we show that ctDNA derived from central nervous system tumours is more abundantly present in the CSF than in plasma. CSF ctDNA can be used to detect brain tumour private mutations and to longitudinally monitor the changes in brain tumour burden. In addition, we provided evidence that the analysis of CSF ctDNA may complement the diagnosis of LC.

Results

CSF ctDNA is representative of brain tumours. To study and compare the ctDNA present in the CSF with plasma ctDNA, we sequenced DNA obtained from tumour samples, germline DNA (peripheral blood lymphocytes), plasma and CSF of a cohort of 12 patients (4 GBM, 6 BMBCs, 2 BMLCs; Supplementary Table 1). In all cases, except BMBCs, CSF was obtained at the same time than plasma through lumbar puncture or cerebral shunts normally obtaining 1–2 ml of CSF. Tumours and fluids from all six cases of BMBCs were obtained through warm autopsy and the CSF was collected from the cisterna magna. We performed targeted capture massively parallel sequencing and, in all cases, somatic single-nucleotide variants (SNVs), insertion/deletions (indels) and copy-number alterations (CNA) were identified in CSF ctDNA and plasma ctDNA, and validated in the brain tumour tissue from the respective patients (Fig 1a,b, Supplementary Figs 1 and 2, Supplementary Tables 2, 3, Supplementary Data 1, 2, 3). The number of genomic alterations identified through targeted capture sequencing varied from case to case being more abundant in BMBCs and less abundant in GBM cases due to the nature of the genes selected for targeted sequencing. A low rate of mutation capture was observed in the CSF ctDNA from GBM patients indicating that further work is required in order to optimize the detection of ctDNA in GBM cases. CSF ctDNA was identified in all cases while plasma ctDNA was only detected in patients with abundant visceral disease. This is in agreement with previous reports[4]. Our methodology exhibits a detection limit of 2% mutant allelic frequency (MAF)[10] and patients with low tumour burden present evidence of plasma ctDNA with MAFs below 2% (ref. 4).

In the case of samples from the autopsy material of patients BMBC2, BMBC3, BMBC4 and BMBC6, we had enough number of specimens to infer phylogenetic trees representing the genomic subclonal diversity and be able to identify trunk ubiquitous genetic mutations. Interestingly, trunk mutations were always identified in the CSF ctDNA (Fig. 1b).

In addition, we sequenced the DNA concomitantly extracted from the CSF and plasma in an expansion cohort of 11 patients (2 Medullos, 5 BMLCs, 4 BMBCs) with CNS restricted disease and barely any visceral tumour burden to facilitate the comparison of the contribution of the brain tumour DNA into the CSF or plasma ctDNA. In all cases, CSF ctDNA was detected and harboured gene mutations that were either absent or detected with lower MAFs in plasma ctDNA (Supplementary Fig. 1).

ctDNA from CSF performs better than plasma. We next sought to determine whether CSF ctDNA would be more representative of the brain lesions than plasma ctDNA. To this end we divided the patients into two groups depending on the amount of extracranial tumour burden (Supplementary Table 4).

Importantly, in patients with a CNS restricted disease (Fig. 1a, Supplementary Fig. 1), the MAFs in all samples of CSF ctDNA were significantly higher than in plasma (Supplementary Fig. 3) and, moreover, the sensitivity for somatic mutations of the CNS was also significantly higher in CSF ctDNA than plasma ctDNA (Fig. 2, Supplementary Table 5). Some mutations were detected in the CSF or plasma but not in the brain tumour specimen (Fig. 1). These could be potential false positives or mutations not present in the sequenced tumour fragment but present in another region of the brain tumour. In patients with abundant visceral disease (Fig. 1b), the MAFs of the gene mutations in the CSF and plasma ctDNA were comparable (Supplementary Fig. 3).

CSF ctDNA recapitulates the private mutations from CNS lesions. We have recently observed that, in the context of disseminated disease, brain metastasis might exhibit private gene mutations different from the ones present in the rest of the tumour lesions[11]. We next investigated how CSF and plasma ctDNA might recapitulate the private mutations from CNS lesions in metastatic patients. To answer this question, we analysed the warm autopsy materials of a patient with Li Fraumeni syndrome and a diagnosis of both HER2-positive metastatic breast cancer and esthesioneuroblastoma (BMBC3). Two sets of tumours were present: the breast cancer-derived brain metastasis and, independently, the meningeal implants and liver metastases (Supplementary Fig. 4). The gene mutations of the brain metastasis were not present in the extracranial tumours and, moreover, we identified three private gene mutations (*PIK3CB* M819L, *PIK3CB* Q818H, *AHNAK2* L5292V) exclusively present in the meningeal lesion. The gene mutations with the highest MAFs of the brain metastasis and the private mutations in the meningeal lesions were present in the CSF ctDNA and not in the plasma ctDNA (Fig. 1b, see boxed mutations) indicating that brain private mutations are more represented in the ctDNA from CSF than plasma.

CSF ctDNA is longitudinally modulated throughout treatments. To address whether the amount of ctDNA present in the CSF could fluctuate with time and be representative of the brain tumour progression, we obtained concomitantly CSF and plasma from six patients (GBM and metastatic breast and lung cancer patients with brain metastasis) at sequential time points (Supplementary Table 1, Fig. 3). In all cases, there was a minimal or absent extracranial disease. Brain lesions were identified using magnetic resonance imaging and brain tumour burden

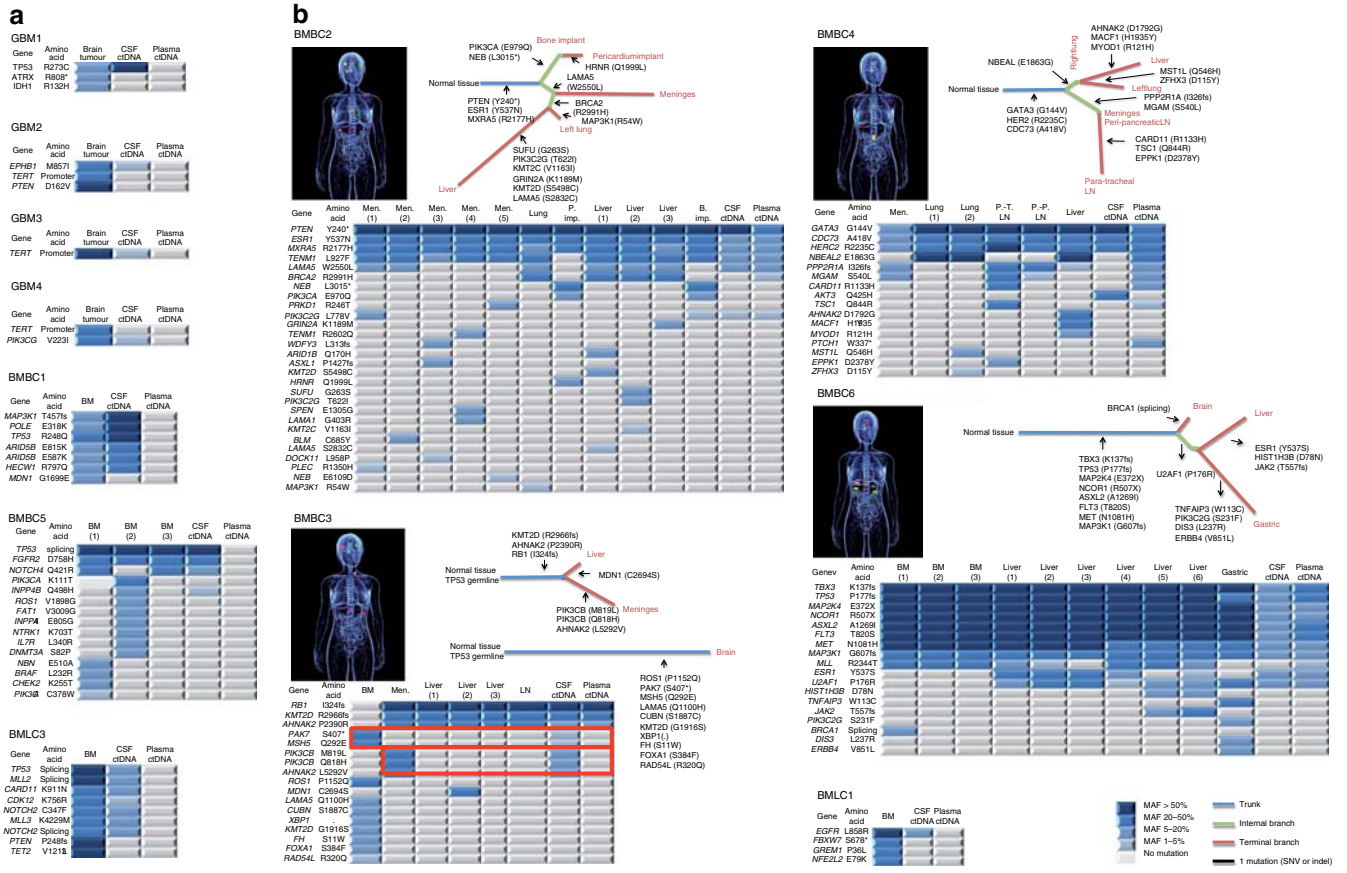

Figure 1 | CSF ctDNA better captures the genomic alterations in patients with brain tumours than plasma ctDNA. (**a**,**b**) Analysis of CSF ctDNA, plasma ctDNA and primary brain tumour or metastatic lesions collected simultaneously. Heatmap of the non-silent genetic alterations from each of the twelve cases is shown and phylogenetic trees of the autopsied patients with brain metastasis from breast cancer (BMBC) are represented. Colour key for mutant allelic frequencies (MAFs) is shown. (**a**) Patients with restricted central nervous system (CNS) disease, glioblastoma (GBM), BMBC and brain metastasis from lung cancer (BMLC). (**b**) Patients with CNS and non-CNS disease. BM, brain metastasis; LN, lymph node; Men, meninges; P. Imp, pericardium implant; PT, para-tracheal; PP, peri-pancreatic.

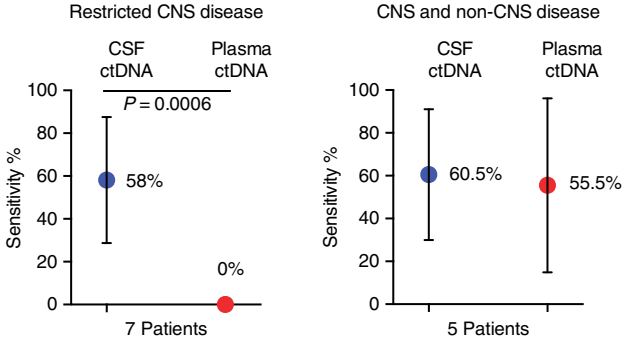

Figure 2 | Sensitivity analysis of CSF ctDNA and plasma ctDNA. Sensitivity was inferred based on gene mutations detected in central nervous system (CNS) tumours, which were either identified in CSF or plasma ctDNA (Supplementary Table 5). Data were pooled and the mean with standard deviation error bars is shown. A Mann–Whitney test was used for the analysis and *P* value is shown.

was quantified using computer aided planimetric analysis (Supplementary Table 6). The tumour somatic genomic alterations, previously identified in the tumours by exome sequencing, were determined in the CSF-derived DNA of the patients through ddPCR (Fig. 3). As expected, the MAFs in all samples of CSF ctDNA were higher than in plasma (Supplementary Table 7). Importantly, MAFs of CSF ctDNA decreased with surgical resection and/or responses to systemic therapy and increased with tumour progression (Fig. 3). The MAFs were modulated over time and followed the same trend as the variation in brain tumour burden. These results indicated that CSF may be a useful biomarker to monitor tumour progression and response to treatment.

CSF ctDNA complements the diagnosis of LC. The identification of CSF ctDNA led us to the hypothesis that cell-free DNA in the CSF could be used as a diagnostic tool for LC. The diagnosis of LC relies on the detection of malignant cells in the CSF of patients with clinical symptoms. Diagnosis of LC is not trivial and its misdiagnosis has important clinical implications. To define whether the analysis of CSF ctDNA can be employed to enhance the sensitivity of the detection of LC by cytopathologic analysis of CSF, we performed standard of care cytopathologic analysis and CSF ctDNA sequencing in the same samples obtained from three breast cancer patients with clinical signs and symptoms suggestive of LC.

Importantly, there were discrepancies between the cytology and our CSF ctDNA analysis (Fig. 4). In BMBC2, although three cytopathologic analyses yielded negative results, we detected ctDNA with MAFs ranging from 20 to 50% in the two CSF samples that were available (Fig. 4). Given that LC was confirmed at the autopsy of BMBC2, our results indicated that the CSF

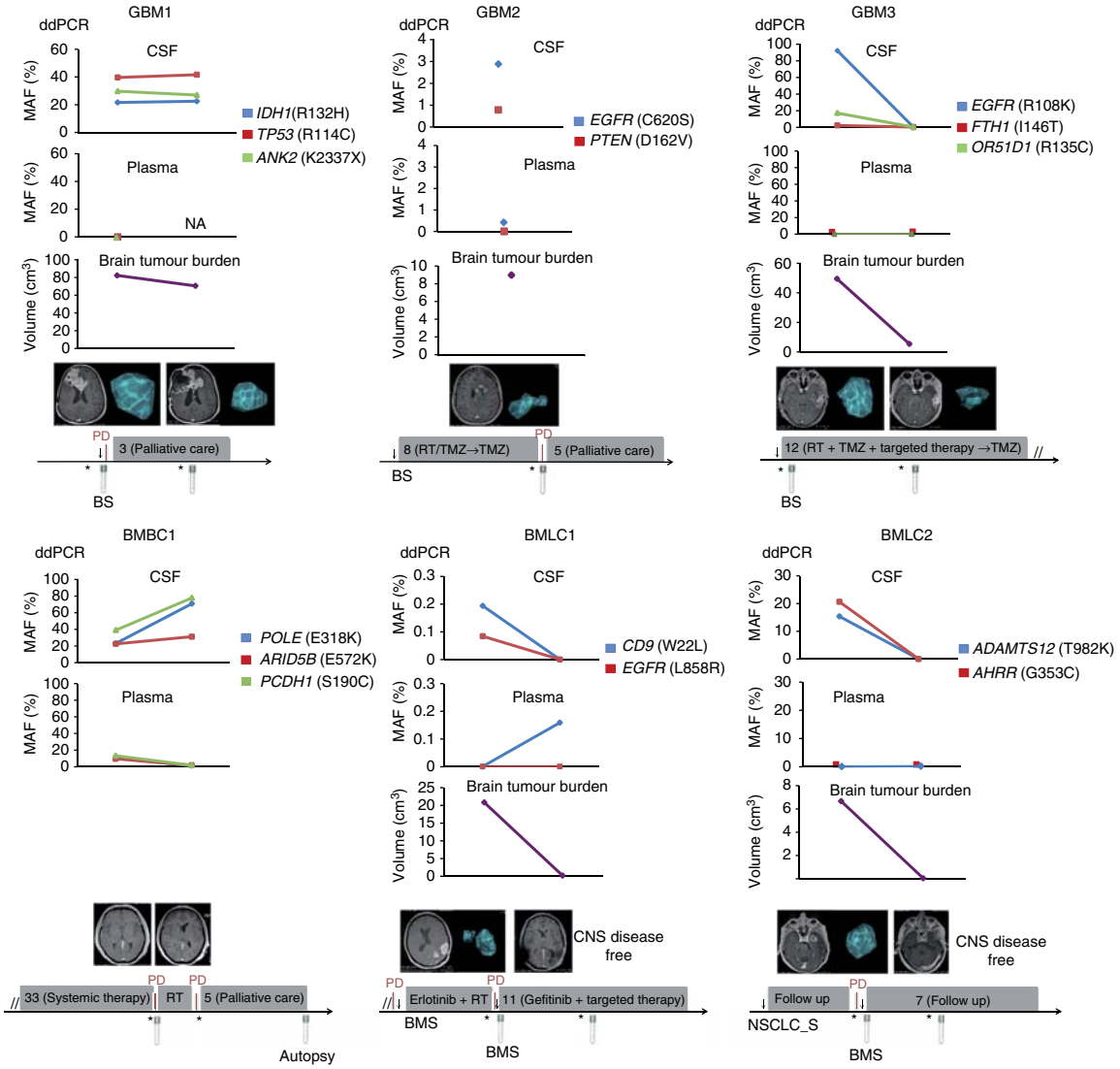

Figure 3 | Dynamic changes in CSF ctDNA recapitulate the treatment courses of patients with brain tumours. Longitudinal monitoring of patients with GBM and brain metastases through CSF and plasma ctDNA and the analysis of brain tumour burden. Gene mutations were measured by ddPCR. Tumour volumes were calculated using computer aided planimetric analysis. Timelines reflect the most relevant clinical information for each patient. BS, brain surgery; BMS, brain metastasis surgery; CNS, central nervous system; NSCLC_S, non-small cell lung cancer surgery; PD, progressive disease; RT, radiotherapy; TMZ, temozolomide. Asterisk and arrow indicate time of magnetic resonance imaging and surgical procedure, respectively. Grey boxes indicate therapy or follow up, and their duration is provided in months.

ctDNA analysis detected disease at a level not detectable by cytopathologic analysis. In BMBC1, one of the cytopathologic analysis was discordant with the presence of CSF ctDNA, while in BMBC4 the results of the cytopathologic analysis and the CSF ctDNA were in agreement. In both cases, BMBC1 and BMBC4, LC was confirmed at the autopsy. In summary, our results build a proof-of-concept that opens the possibility to use CSF ctDNA to complement the diagnosis of LC. Of note, in the case of patients with brain metastasis and clinical signs suggestive of LC, the analysis of CSF ctDNA can be misleading since it will be difficult to discern whether the ctDNA in the CSF is originated from the LC or the brain metastasis. Further studies will be needed to consolidate this methodology for LC diagnosis.

Discussion

In this study, we identified and characterized ctDNA in the CSF of patients with brain lesions and compared it with plasma ctDNA. We showed that CSF ctDNA is more representative of brain tumour genomic alterations than plasma and putative actionable gene mutations and CNA (that is, *EGFR*, *PTEN*, *ESR1*, *IDH1*, *ERBB2*, *FGFR2*) can be identified. We observed that CSF ctDNA has a significantly higher sensitivity than plasma for CNS genomic alterations and can be used to detect brain tumour private mutations and to monitor brain tumour progression. In addition, we provided evidence that the analysis of CSF ctDNA may complement the diagnosis of LC.

One of the hallmarks of GBM is the fact that all tumours relapse. Once diagnosed, the GBM tumour is surgically resected and then the patient receives radio- and chemotherapy treatments. Even when the surgical resection is complete, the tumour invariably relapses. Importantly, the relapsed tumour tends to evolve under treatment and present different genomic alterations than the primary tumour[12]. Surgical procedures (resection and biopsies) are seldom indicated in relapsed GBM limiting its genomic characterization and precluding the treatment of the relapsed GBM based on genomic information. CSF ctDNA provides a minimally invasive method to assess the

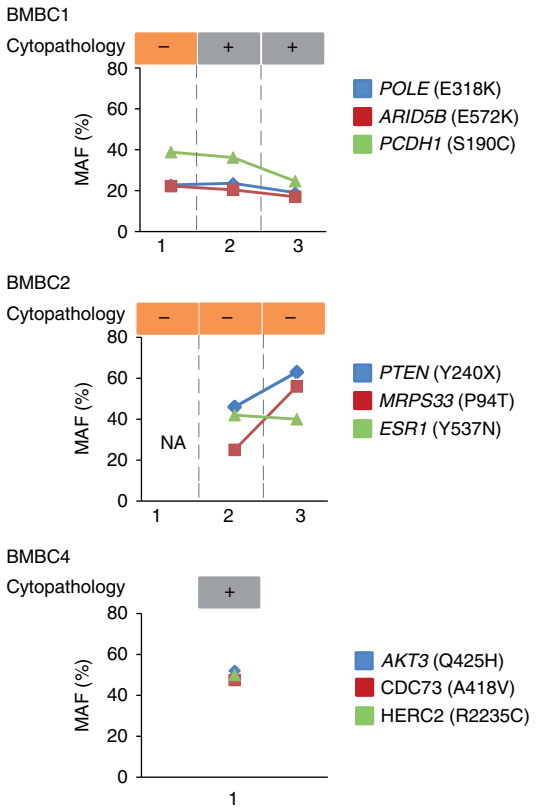

Figure 4 | Analysis of CSF ctDNA as a diagnostic tool for leptomeningeal carcinomatosis in three metastatic breast cancer patients. The results of serial clinical cytopathology analyses are shown in the upper part of the graph. In the lower part, mutant allelic frequencies (MAFs) measured by ddPCR in the same CSF samples are depicted. NA, not available.

genomic alterations of the relapsed tumour helping to select the optimal treatment dictated by the molecular characteristics of the brain cancer.

On the other hand, patients with brain metastasis exhibit a dismal prognosis and are usually recalcitrant to treatments. It is known that, most likely due to the special environment of the brain, the genomic alterations of brain metastasis differ from the ones of the visceral malignancies and primary tumours[11–15]. The identification of the brain metastasis-specific genomic alterations through CSF ctDNA might facilitate the design of tailored treatments to target brain metastasis hopefully increasing the clinical response of these deadly lesions.

In a context where the oncology field expects that therapeutic approaches will be dictated and guided by the genomic features of tumours, the presence of CSF ctDNA will be fundamental to the correct molecular diagnosis and treatment of brain tumours. Altogether, our results indicate that CSF ctDNA can be exploited as a 'liquid biopsy' of brain tumours opening a novel avenue of research in CNS circulating biomarkers with an important impact in the future characterization, diagnosis, prognosis and clinical managing of brain cancer.

Methods

Patients. Breast cancer patients with brain metastasis were enrolled as part of the Vall d'Hebron Institute of Oncology (VHIO) Warm Autopsy Program. Patients with breast cancer and lung cancer with brain metastasis, and GBM and medulloblastoma were enrolled as part of VHIO Prospective Translational Program, which studies plasma and CSF-derived biomarkers. Patients with lung cancer with brain metastasis were enrolled as part a collaborative effort with Dexeus University Hospital (Barcelona, Spain) and the research was approved by the local institutional review board (IRB)/ethics committee of both hospitals. VHIO Warm Autopsy Program and the Prospective Translational Program were approved by the IRB of Vall d'Hebron University Hospital (Barcelona, Spain). Informed consent was obtained from all patients.

DNA extraction. The diagnosis of each metastatic lesion was confirmed on review of routine hematoxylin and eosin-stained slides[6]. Ten 8-μm thick sections from representative fresh frozen metastasis biopsies/resections were cut, stained with nuclear fast red and microdissected with a needle under a stereomicroscope to ensure >80% of tumour cell content, as previously described[16]. DNA from microdissected tumour samples was extracted using DNeasy Blood and Tissue Kit (Qiagen, USA), and germline DNA from peripheral blood lymphocytes ('buffy coat') was extracted using the QIAamp DNA Mini Kit (Qiagen) according to manufacturer's instructions. CSF-derived and plasma-derived circulating cell-free DNA was extracted with the QIAamp Circulating Nucleic Acid Kit (Qiagen, Valencia, CA, USA), as previously described[6]. DNA was quantified using the Qubit Fluorometer (Invitrogen).

Targeted capture massively parallel sequencing. DNA samples from CNS tumours (primary brain tumours or CNS metastases) of 23 cases, non-CNS metastases, CSF and plasma samples as well as germline DNA were subjected to targeted capture massively parallel sequencing at the Memorial Sloan Kettering Cancer Center Integrated Genomics Operation (iGO), using the Integrated Mutation Profiling of Actionable Cancer Targets (MSK-IMPACT) platform[17] targeting all exons of 341 cancer genes harbouring actionable mutations. For four additional cases with breast cancer and brain metastases (BMBC1-4) were analysed with a customized breast cancer panel, targeting all exons of 254 genes recurrently mutated in breast cancer and/or related to DNA repair (Supplementary Data 1) was also performed. For these four cases, of the 595 genes captured, 107 genes were common to both targeted capture platforms (that is, 488 unique genes), and were employed for validation. By applying the methods described above to each targeted capture platform independently, the validation rate of somatic mutations (SNVs and indels) affecting the exons of 107 genes present in both platforms was >96% (Supplementary Table 3).

Targeted sequencing was performed as previously described[6,17,18]. In brief, 20–450ng of DNA was used to prepare barcoded sequence libraries (New England Biolabs, Kapa Biosystems), which were pooled at equimolar concentrations for hybridization exon capture (Nimblegen SeqCap).

Paired-end 100-bp reads were generated on the Illumina HiSeq2000 (San Diego, CA), and reads were aligned to the reference human genome hg19 using the Burrows-Wheeler Aligner[19]. Local realignment, duplicate removal and base quality recalibration were performed using the Genome Analysis Toolkit[20]. Somatic SNVs were called using MuTect[21], and small insertions and deletions (indels) were called using Strelka[22], VarScan 2 (ref. 23) and SomaticIndelDetector[17]. All candidate mutations were reviewed manually using the Integrative Genomics Viewer[24]. Somatic mutations with allelic fractions of <1% and/or supported by <2 reads were disregarded. The mean sequence coverage of each target exon was subjected to a loess normalization to adjust for bias in nucleotide composition (G+C) and compared with the diploid normal sample. Gene copy-number profiles were generated using circular binary segmentation[17].

Exome sequencing of tumour DNA and normal DNA. DNA (500ng) extracted from brain tumour and germline samples from GBM1, GBM2 and GBM3, BMBC1, BMLC1 and BMLC2 cases were subjected to exome sequencing. An average of 100 million 100-bp paired-end reads were generated for each sample, equivalent to an average depth of 260× (range of 190–315×). Exome sequencing was performed using the Nextera Rapid Capture Exome kit (37 Mb; Illumina) on an Illumina HiSeq 2000 instrument using a validated protocol[25] and according to the manufacturer's recommendations (Macrogen).

ddPCR and quantification of circulating tumour-specific DNA. ddPCR of plasma and CSF were performed using the QX200 Droplet Digital PCR system (Bio-Rad) according to manufacturer's protocols and the literature[26]. TaqMan-based quantitative PCR assays were designed to specifically detect point mutations and corresponding wild-type alleles as selected by exome sequencing of primary brain tumours or brain metastases. Primer sequences are provided in Supplementary Table 8. Ten nanograms of genomic DNA extracted from tumour tissue and germline DNA from peripheral blood lymphocytes was used for digital PCR analysis. In some cases, lower amounts of DNA (for example, 1–5 ng) were used, due to CSF and plasma DNA yield limitations.

The phylogenetic tree generation. Phylogenetic trees were constructed using the maximum parsimony method. The trunks of the trees were rooted by a germline DNA sequence that did not have any of the somatic mutations. Trunk, branch and sub-branches lengths are proportional to the number of mutations.

Statistical analysis. A Mann–Whitney test was performed for statistical analysis. Data in graphs are presented as means ± s.d.

References

1. Gerlinger, M. *et al.* Intratumor heterogeneity and branched evolution revealed by multiregion sequencing. *N. Engl. J. Med.* **366,** 883–892 (2012).
2. Sottoriva, A. *et al.* Intratumor heterogeneity in human glioblastoma reflects cancer evolutionary dynamics. *Proc. Natl Acad. Sci. USA* **110,** 4009–4014 (2013).
3. Omuro, A. & DeAngelis, L. M. Glioblastoma and other malignant gliomas: a clinical review. *JAMA* **310,** 1842–1850 (2013).
4. Murtaza, M. *et al.* Non-invasive analysis of acquired resistance to cancer therapy by sequencing of plasma DNA. *Nature* **497,** 108–112 (2013).
5. Dawson, S. J. *et al.* Analysis of circulating tumor DNA to monitor metastatic breast cancer. *N. Engl. J. Med.* **368,** 1199–1209 (2013).
6. De Mattos-Arruda, L. *et al.* Capturing intra-tumor genetic heterogeneity by de novo mutation profiling of circulating cell-free tumor DNA: a proof-of-principle. *Ann. Oncol.* **25,** 1729–1735 (2014).
7. Bettegowda, C. *et al.* Detection of circulating tumor DNA in early- and late-stage human malignancies. *Sci. Transl. Med.* **6,** 224ra24 (2014).
8. Segal, M. B. Extracellular and cerebrospinal fluids. *J. Inherit. Metab. Dis.* **16,** 617–638 (1993).
9. Pan, W., Gu, W., Nagpal, S., Gephart, M. H. & Quake, S. R. Brain tumor mutations detected in cerebral spinal fluid. *Clin. Chem.* **61,** 514–522 (2015).
10. Cheng, D. T. *et al.* Memorial sloan kettering-integrated mutation profiling of actionable cancer targets (MSK-IMPACT): a hybridization capture-based next-generation sequencing clinical assay for solid tumor molecular oncology. *J. Mol. Diagn.* **17,** 251–264 (2015).
11. Brastianos, P. K. *et al.* Genomic characterization of brain metastasis reveals branched evolution and potential therapeutic targets. *Cancer Discov.* **5,** 1–14 (2015).
12. Johnson, B. E. *et al.* Mutational analysis reveals the origin and therapy-driven evolution of recurrent glioma. *Science* **343,** 189–193 (2014).
13. Ding, L. *et al.* Genome remodelling in a basal-like breast cancer metastasis and xenograft. *Nature* **464,** 999–1005 (2010).
14. Saunus, J. M. *et al.* Integrated genomic and transcriptomic analysis of human brain metastases identifies alterations of potential clinical significance. *J. Pathol.* **237,** 363–378 (2015).
15. Paik, P. K. *et al.* Next-generation sequencing of stage IV squamous cell lung cancers reveals an association of PI3K aberrations and evidence of clonal heterogeneity in patients with brain metastases. *Cancer Discov.* **5,** 610–621 (2015).
16. Hernandez, L. *et al.* Genomic and mutational profiling of ductal carcinomas in situ and matched adjacent invasive breast cancers reveals intra-tumour genetic heterogeneity and clonal selection. *J. Pathol.* **227,** 42–52 (2012).
17. Won, H. H., Scott, S. N., Brannon, A. R., Shah, R. H. & Berger, M. F. Detecting somatic genetic alterations in tumor specimens by exon capture and massively parallel sequencing. *J. Vis. Exp.* **80,** e50710 (2013).
18. Natrajan, R. *et al.* Characterization of the genomic features and expressed fusion genes in micropapillary carcinomas of the breast. *J. Pathol.* **232,** 553–565 (2014).
19. Li, H. & Durbin, R. Fast and accurate short read alignment with Burrows-Wheeler transform. *Bioinformatics* **25,** 1754–1760 (2009).
20. DePristo, M. A. *et al.* A framework for variation discovery and genotyping using next-generation DNA sequencing data. *Nat. Genet.* **43,** 491–498 (2011).
21. Cibulskis, K. *et al.* Sensitive detection of somatic point mutations in impure and heterogeneous cancer samples. *Nat. Biotechnol.* **31,** 213–219 (2013).
22. Saunders, C. T. *et al.* Strelka: accurate somatic small-variant calling from sequenced tumor-normal sample pairs. *Bioinformatics* **28,** 1811–1817 (2012).
23. Koboldt, D. C. *et al.* VarScan 2: somatic mutation and copy number alteration discovery in cancer by exome sequencing. *Genome Res.* **22,** 568–576 (2012).
24. Robinson, J. T. *et al.* Integrative genomics viewer. *Nat. Biotechnol.* **29,** 24–26 (2011).
25. Lamble, S. *et al.* Improved workflows for high throughput library preparation using the transposome-based Nextera system. *BMC Biotechnol.* **13,** 104 (2013).
26. Forshew, T. *et al.* Noninvasive identification and monitoring of cancer mutations by targeted deep sequencing of plasma DNA. *Sci. Transl. Med.* **4,** 136ra68 (2012).

Acknowledgements

We thank all the patients and their families that participated in this study. The authors acknowledge Fundación Rafael del Pino for financial support (for L. De Mattos-Arruda) and the ERC grant (Glioma), Asociación Española contra el Cáncer (AECC), the Josef Steiner Foundation, FIS PI13/02661 and the FERO and Cellex foundation.

Author contributions

J.S. designed the study. L.D.M.-A., F.M.-R., D.T., M.O., J.R., J.Ca., M.G.-C., E.F., J.Ta., E.F., J.Sa., J.C. contributed with patients. L.D.M.-A., R.M., C.K.Y.N., B.W., A.A., C.R., J.T., E.G.-R, E.M.-R., S.P., R.T., V.P., S.J.C. developed methods. L.D.M.-A., R.M., C.K.Y.N. generated data. S.L., O.M., X.C., A.V., J.S.R.-F., J.Ta., M.F.B. contributed sequencing data. L.D.M.-A., C.K.Y.N., B.W., M.F.B., J.S.R.-F., J.S. analysed sequencing data. L.D.M.-A., J.S.R.-F, J.C., J.S. interpreted the data. J.S wrote the paper with assistance of L.D.M.-A. and the other authors. All authors approved the final manuscript.

Additional information

Accession codes: Whole-exome and targeted capture massively parallel sequencing have been deposited in the Sequence Read Archive (SRA) under accession code SRP049647.

Supplementary Information accompanies this paper at http://www.nature.com/naturecommunications

Competing financial interests: The authors declare no competing financial interests.

Reprints and permission information is available online at http://npg.nature.com/reprintsandpermissions/

How to cite this article: De Mattos-Arruda, L. *et al.* Cerebrospinal fluid-derived circulating tumour DNA better represents the genomic alterations of brain tumours than plasma. *Nat. Commun.* 6:8839 doi: 10.1038/ncomms9839 (2015).